NCPA Optimizations at Gemini North using Focal Plane Sharpening

by

Jesse Ball

A Thesis Submitted to the Faculty of the

COLLEGE OF OPTICAL SCIENCES

In Partial Fulfillment of the Requirements

For the Degree of

MASTER OF SCIENCE

In the Graduate College

THE UNIVERSITY OF ARIZONA

May 5, 2016

STATEMENT BY AUTHOR

The thesis titled *NCPA Optimizations at Gemini North using Focal Plane Sharpening* prepared by *Jesse Ball* has been submitted in partial fulfillment of requirements for a master's degree at the University of Arizona and is deposited in the University Library to be made available to borrowers under rules of the Library.

Brief quotations from this thesis are allowable without special permission, provided that an accurate acknowledgement of the source is made. Requests for permission for extended quotation from or reproduction of this manuscript in whole or in part may be granted by the head of the major department or the Dean of the Graduate College when in his or her judgment the proposed use of the material is in the interests of scholarship. In all other instances, however, permission must be obtained from the author.

SIGNED: _____
Jesse Ball

APPROVAL BY THESIS DIRECTOR

This thesis has been approved on the date shown below:

_____   05 May, 2016
Jose Sasian   *Date*
Professor of Optical Sciences

ACKNOWLEDGEMENTS

Contents

List of Figures

List of Tables

Abstract

Non-common path aberrations (NCPA) in an adaptive optics system are static aberrations that appear due to the difference in optical path between light arriving at the wavefront sensor (WFS) and at the science detector. If the adaptive optics are calibrated to output an unaberrated wavefront, then any optics outside the path of the light arriving at the WFS inherently introduce aberrations to this corrected wavefront. NCPA corrections calibrate the adaptive optics system such that it outputs a wavefront that is inverse in phase to the aberrations introduced by these non-common path optics, and therefore arrives unaberrated at the science detector, rather than at the output of the corrective elements.

Focal plane sharpening (FPS) is one technique used to calibrate for NCPA in adaptive optics systems. Small changes in shape to the deformable element(s) are implemented and images are taken and analyzed for image quality (IQ) on the science detector. This process is iterated until the image quality is maximized and hence the NCPA are corrected.

The work carried out as described in this paper employs two FPS techniques at Gemini North to attempt to mitigate up to 33% of the adaptive optics performance and image quality degradations currently under investigation. Changes in the NCPA correction are made by varying the Zernike polynomial coefficients in the closed-loop correction file for Altair (the facility adaptive optics system). As these coefficients are varied during closed-loop operation, a calibration point-source at the focal plane of the telescope is imaged through Altair and NIRI (the facility near-infrared imager) at f/32 in K-prime ($2.12~\mu m$). These images are analyzed to determine the Strehl ratio, and a parabolic fit is used to determine the appropriate coefficient correction that maximizes the Strehl ratio.

Historic calibrations of the NCPA file in Altair's control loop were done at night on a celestial point source, and used a separate, high-resolution WFS (with its own inherent aberrations not common to either NIRI nor Altair) to measure phase corrections directly. In this paper it is shown that using FPS on a calibration source negates both the need to use costly time on the night sky and the use of separate optical systems (which introduce their own NCPA) for analysis. An increase of 6% in Strehl ratio is achieved (an improvement over current NCPA corrections of 11%), and discussions of future improvements and extensions of the technique is presented. Furthermore, a potentially unknown problem is uncovered in the form of high spatial frequency degradation in the PSF of the calibration source.

1 Overview of Adaptive Optics at Gemini North

A brief overview of atmospheric turbulence and adaptive optics with a Shack-Hartman wavefront sensor is presented as context for the study conducted in this paper.

1.1 Atmospheric Turbulence and the need for Adaptive Optics

The atmosphere distorts the propagation of light much in the same way turbulent water does (although not so drastically). Albeit a small one, the air above the planet does have an index of refraction slightly bigger than 1 (vacuum), and it varies proportionately to temperature fluctuations. These variations can be modeled fairly well on local time and distance scales by the "Komolgorov-Obukhov law of turbulence" and can be expressed by both spatial and temporal index structure functions. These functions basically describe a how turbulent atmosphere with "pockets" of various sizes (spatial component) of different temperatures, moving over time (temporal component) due to wind sheer affect[1] the local index of refraction. We usually assume that light from a star forms at infinity and by the time it reaches the earth's atmosphere its wavefront can be assumed to be planar (i.e., the phase of the propagating wave is constant over the span of a plane). As the plane wave traverses these pockets of turbulence with varying indices of refraction, different locations on the incoming wavefront will be aberrated in different manners, naturally: in effect, the phase over an area larger than the turbulent pockets will no longer lie on the same plane. By the time the light reaches an observer on the ground, the incoming wavefront is no longer planar, and therefore naturally produces a "blur" when this light passes through an imaging system. Astronomers refer to this blur as "seeing."

When projected to a two-dimensional plane at the aperture of the telescope, the *index* structure functions can be expressed as *phase* structure functions [2].

$$D_\phi(\Delta \mathbf{r}) = 6.88(\Delta \mathbf{r}/r_0)^{5/3}, \text{ where } \Delta \mathbf{r} = \bar{\nu}\tau$$

Here, Δr is a displacement vector from one point on the pupil to another,

---

[1]The time it takes for temperature to vary in any given spot is much less than the time it takes wind to push another pocket of turbulence to/ from that spot [2].

and can be expressed temorally in terms of the average velocity, $\bar{\nu}$, of the wind sheers above the observation point, and a displacement in time, τ; which is known as the Taylor approximation and is reflects the fact that the changes in temperature that are not dependent on wind speed are negligible. Here, r_0 is known as the Fried parameter and is a *measurement* of the local inhomogeneities in index of refraction: it represents the diameter of a circular area over which the turbulent atmosphere disrupts the phase of a wavefront by 1 radian rms. The Fried parameter is related to the air mass (or zenith angle, γ), the wavelength ($\lambda = 2\pi/k$), and an *index structure coefficient*, C_N^2, that depends on height and represents the *strength* of the local inhomogeneities.[2]

$$r_0 \approx \left[0.423 k^2 (\cos\gamma)^{-1} \int C_N^2(h) \mathrm{d}h \right]^{-3/5}$$

To summarize, r_0 is a measurement estimate of the area over which a wavefront will be notably distorted, and C_N^2 characterizes the intensity of the seeing. Similarly, a parameter $\tau_0 = r_0/\bar{v}$ characterizes the temporal coherence of the atmosphere. It is both r_0 and τ_0 that determine the necessary corrections needed for an optical system with a given entrance pupil diameter.

For large, ground-based telescopes, turbulence is a fundamental limitation of the image quality. The resolution of a diffraction-limited imaging system, $\alpha_{Rayleigh} \approx 1.22\lambda/D$, is dependent on the diameter of the entrance pupil: the bigger the telescope, the smaller (i.e., better) the angular resolution. However, as mentioned above the Fried parameter describes the diameter of local inhomogeneities in the index of refraction, and is on the order of 10-20 cm in most sites dedicated to astronomical telescopes (even smaller in less stable sites). Since the diameter of a large, ground-based telescope is much larger than this, the (uncorrected) image quality is necessarily and significantly limited by the atmospheric turbulence and is only resolved on the order of λ/r_0. Another way to look at it is that when turbulent cells are smaller than the entrance aperture, the blurring effects themselves are well-resolved on short spatial (and/ or temporal) scales, causing a degradation in image quality, as the phase over the entire entrance pupil is projected to the image plane. This is why smaller telescopes are not as affected by the turbulence: the aperture of such a telescope is on the order of (or smaller than) the coherence length of the turbulence, and therefore has a relatively constant phase over the pupil (although the resolution is now limited by the Rayleigh criterion mentioned above).

Due to the high resolution of large diameter telescopes and their relative size compared with turbulent cells, methods to alleviate these dynamic aberrations due to atmospheric turbulence must be invoked. *Adaptive optics* have been developing since the mid 1950s to do just that. In general, adaptive optics consist of some sort of rapidly deformable element (DM) that can be shaped such that the phase variations introduced by the turbulence are "flattened" by the shape of the optic(s). The incoming light is imaged onto a detector which rapidly[2] reads and analyzes the signal and sends demands to the deformable element that will shape the outgoing wavefront and deliver this "flattened" wave to a science instrument. In effect, adaptive optics strive to cancel the effects of the variable index of refraction due to turbulence in the atmosphere.

1.2   The Shack-Hartmann Wavefront Sensor

There are many different ways to configure an adaptive optics system, including curvature sensors, pyramid sensors, and Shack-Hartmann sensors, among others. Gemini North's adaptive optics facility, Altair, uses the Shack-Hartmann configuration. In this configuration, incoming light passes though a deformable element, usually consisting of a deformable mirror and a separate tip/ tilt mirror that handles lower-order aberrations, and is split by a dichroic element such that the longer (near-infrared) wavelengths are passed on to a science detector and the shorter (visible) wavelengths are sent through an array of lenslets at a pupil plane and imaged onto a separate detector. Each lenslet images the source from a portion of the wavefront in the pupil plane, so that the detector sees an array of (point) images. The detector is divided into sub-apertures, a grid of boxes, that surround these point-source images. In principle, the lateral displacement, ε, of an incoming wavefront on the focal plane (detector) is related to the derivative (slope) of the phase[3], ϕ, at the pupil by the following displacement-slope relationship:

$$\varepsilon_Y \approx -\frac{2f}{d}\frac{\partial\phi}{\partial y}$$

---

[2]The correction process for AO systems must be on the order of or faster than the coherence time τ_0 over which the atmosphere distorts the phase appreciably. This is, of course, dependent both on wavelength and wind speed, but is on the order of tens to hundreds of milliseconds.

[3]In the field of astronomical adaptive optics, the amplitude component is usually dropped from the wavefront distribution due to its negligible relative contribution to rms variations in the wavefront through atmospheric turbulence[2].

$$\varepsilon_x \approx -\frac{2f}{d}\frac{\partial \phi}{\partial x},$$

where f and d are the focal length and diameter of the lenslet, respectively. This fundamental relationship simply shows that the positions of the spots on the wavefront sensor's detector exhibit a linear relationship with respect to the phase at the pupil. Therefore, the phase can be manipulated (working backwards) to put the spots back on their ideal centroids (a square grid of spots for a flat wavefront). This is done empirically in the case of a Shack-Hartman WFS by measuring the centroids and applying movements to the DM in order to move the centroids back to their ideal position on the WFS through a process known as *wavefront reconstruction*.

The centroids can be calculated in various ways on various types of detectors. In the case of Altair at Gemini North, it is determined using *quad-cells*. Quad cells consist of four sub-apertures on the focal plane (e.g., 4 pixels in a CCD) on which the spot of an unaberrated source lands directly in the middle: there are one set of quad-cells in the focal plane per lenslet in the pupil, and they are well separated both by a row and column of "guard cells" that are not read out so as to mitigate cross-talk effects[12]. The centroid offset (i.e., the displacement ε) is then calculated using the relative intensity detected on each of these cells (Figure 1). The main advantage of using a quad-cell detector for centroiding is that it is extremely fast to read out and to calculate compared with oversampling on a normal CCD. A drawback is that the centroid is under-sampled and relies heavily upon a gain factor that is determined by the size of the spot, which changes due to local seeing conditions and/ or when correcting extended sources such as moons, asteroids, and galactic cores. This gain factor, in Altair, is determined and accounted for within the control loops[11].

Because of the aforementioned linear relationship, the measured centroids in the focal plane of the lenslets, in effect, are representative of the phase in the pupil plane and thus can be used to manipulate the DM's shape such that the phase is cancelled and thus the wavefront is flattened. In practice this phase reconstruction calculation is done by first calibrating an *interaction matrix, C*, that represents the response of the deformable mirror to movement of its actuators (somewhat analogous to the operations on the right side of the displacement-slope relationships shown above). To create this matrix, voltages are applied empirically to the actuators, a, and measurements, m, of the centroid

12

$$\varepsilon_x = r_s \frac{(I_2 - I_1) + (I_3 - I_4)}{\Sigma I}$$

$$\varepsilon_y = r_s \frac{(I_1 - I_4) + (I_2 - I_3)}{\Sigma I}$$
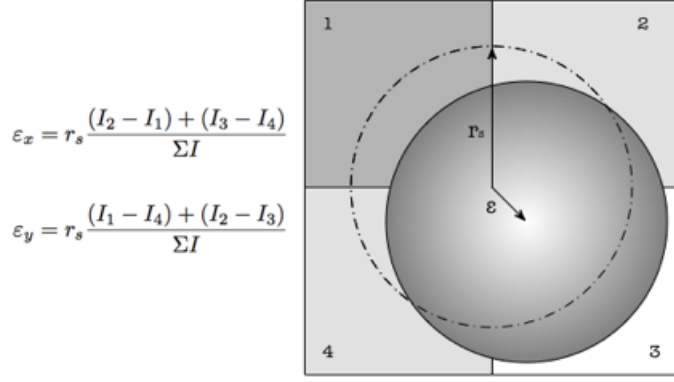
Figure 1: Quad-cell on a Shack-Hartman WFS. The relative intensities of each cell are used to calculate the centroid given a known spot diameter. In the equations above, r_s is the radius of the spot, I_n are the intensities measured in each individual cell, and ΣI is the total intensity measured in the quad-cell. Note that this relationship holds only if the displacement ε, is much smaller than the angular spot size, r_s[8].

offsets are taken.

$$m = Ca,$$

Using this interaction matrix, a *reconstructor matrix, R,* is calculated that is effectively the inverse (or more precisely the pseudo-inverse) of the interaction matrix, C.

$$a = Rm$$

This reconstructor matrix then generates demands for the actuators to flatten the wavefront based on the measurements of (new) centroids on the WFS. Note that the interaction matrix, C, is in practice not square and hence can not be directly inverted; thus the reconstructor R is usually derived using a singular value decomposition techniques on the interaction matrix, and very small singular values that represent "invisible" modes (piston, waffle, etc.) are filtered out. The reconstructor matrix can then be used to interact with the real-time, quad-cell centroid measurements, m, in order to calculate the actuator offset positions, which are then corrected by applying voltages to the DM that send the spots back to their ideal position on the WFS. This wavefront reconstruc-

13

tion and correction process is iterated at a very high frequency (depending on the closed-loop gain values, up to about a tenth of the sampling frequency) so that the correction is being made on a time scale shorter than or equal to the limiting time scale over which the atmospheric distortion changes appreciably (τ_0).

1.3 The NCPA Problem

Aberrations from an ideal, diffraction-limited image are not only introduced by the atmosphere, but by curvatures and alignments in the elements of optical systems themselves. Although major astronomical observatories certainly design their systems to minimize these inherent aberrations, they cannot be completely eliminated. Therefore, after an adaptive optics system corrects for the atmospheric turbulence and any aberrations in its light path[4], the optics between the deformable element and the science detector will introduce their own aberrations to the corrected wavefront. In adaptive optics systems, the light path(s) *after* the beam-splitter traverse distinctly separate optical elements and represent the "non-common path(s)." In order to "provide the best image quality possible from the ground for telescopes of their size[5]," Gemini must attempt to minimize not only atmospheric aberrations, but also these static, non-common path aberrations (NCPA). One way to do this is to use the adaptive optics system to provide the science instrument with a wavefront whose phase is aberrated inversely to that introduced by its own optical system's deterministic aberrations, rather than simply outputting a "flattened" wavefront from the DM. This can be done by changing the ideal centroids on the WFS such that the "best" arrangement of centroids on the WFS is no longer a regular grid, but one which represents lateral displacements ε that correspond to the wavefront distribution that is inverse in phase to these aberrations that are characteristic of the non-common path optics in the system. This NCPA offset, a_{NCPA}, can be added to the reconstructor as a static voltage offset in actuators.

$$a = Rm + a_{NCPA}$$

---

[4]Although not discussed, it should be obvious that since we use empirical centroids, all aberrations between the source and the WFS are accounted for, and not just the atmospheric turbulence (although the turbulence certainly represents the majority).

[5]This is one of Gemini's two principle performance goals when the telescopes were first built[7].

This is the main principle behind this project, in which the NCPA corrections to NIRI, Gemini North's near infrared imaging instrument, are optimized by inserting a static correction to the Altair control loop.

An overview of the principles from sections 1.1 through 1.3 are illustrated in Figure 2. Light from a distant point source travels through the vacuum of space to arrive essentially as a propagating plane wave at Earth's atmosphere. This light then travels through turbulent cells with varying indices of refraction which cause parts of the wavefront to travel at varying speeds, resulting in an aberrated wavefront at the entrance pupil of the telescope (purple; common-path). These aberrations are seen through a Shack-Hartman wavefront sensor as lateral displacements on a quad-cell detector through an array of lenslets, which are converted via a reconstruction matrix into actuator displacements on a deformable mirror. Since the difference in light path through the adaptive optics and the science instrument (blue and red, respectively; non-common path) introduce aberrations that are unaccounted for at the wavefront sensor, a static correction to these non-common path aberrations must be applied to the reconstruction algorithm in order to output a wavefront that is inverse in phase to that of the combined non-common path optics such that light arriving at the imaging plane will be fully corrected. Note that if the NCPA correction is not applied (as in the case with the traditional Shack-Hartman configuration discussed in section 1.2), the light coming out of the adaptive optics system will exhibit a nearly flat wavefront which is then re-aberrated by the non-common path optics (black, inset).

1.4 Overview of Gemini's Telescope, NIRI, and Altair

Before delving into the details of the experiment, a very brief overview of the telescope, instruments, and systems involved is presented[7].

The Telescope

The Gemini North Observatory is located near the summit of Mauna Kea on the Big Island of Hawai'i. It is one of two twin telescopes, the other located on Cerro Pachón outside of La Serena, Chile.

The primary mirror is an f/1.8 convex paraboloid that is 8.1m in diameter and coupled with 120 hydraulic actuators that sit under it, providing active correction both for gravitational distortion due to its own weight and for low-

Figure 2: Adaptive Optics and NCPA Overview

Radiating point source (in vacuum)

Atmosphereic Turbulence

Telescope entrance pupil (aperture)

Telescope focal plane

Deformable optics

AO Control Loops

Dichroic beamsplitter

Shack-Hartmann wavefront sensor

Instrument's optics

NCPA-corrected science light path

Science light path from AO system not corrected for NCPA

Science Detector (image plane)
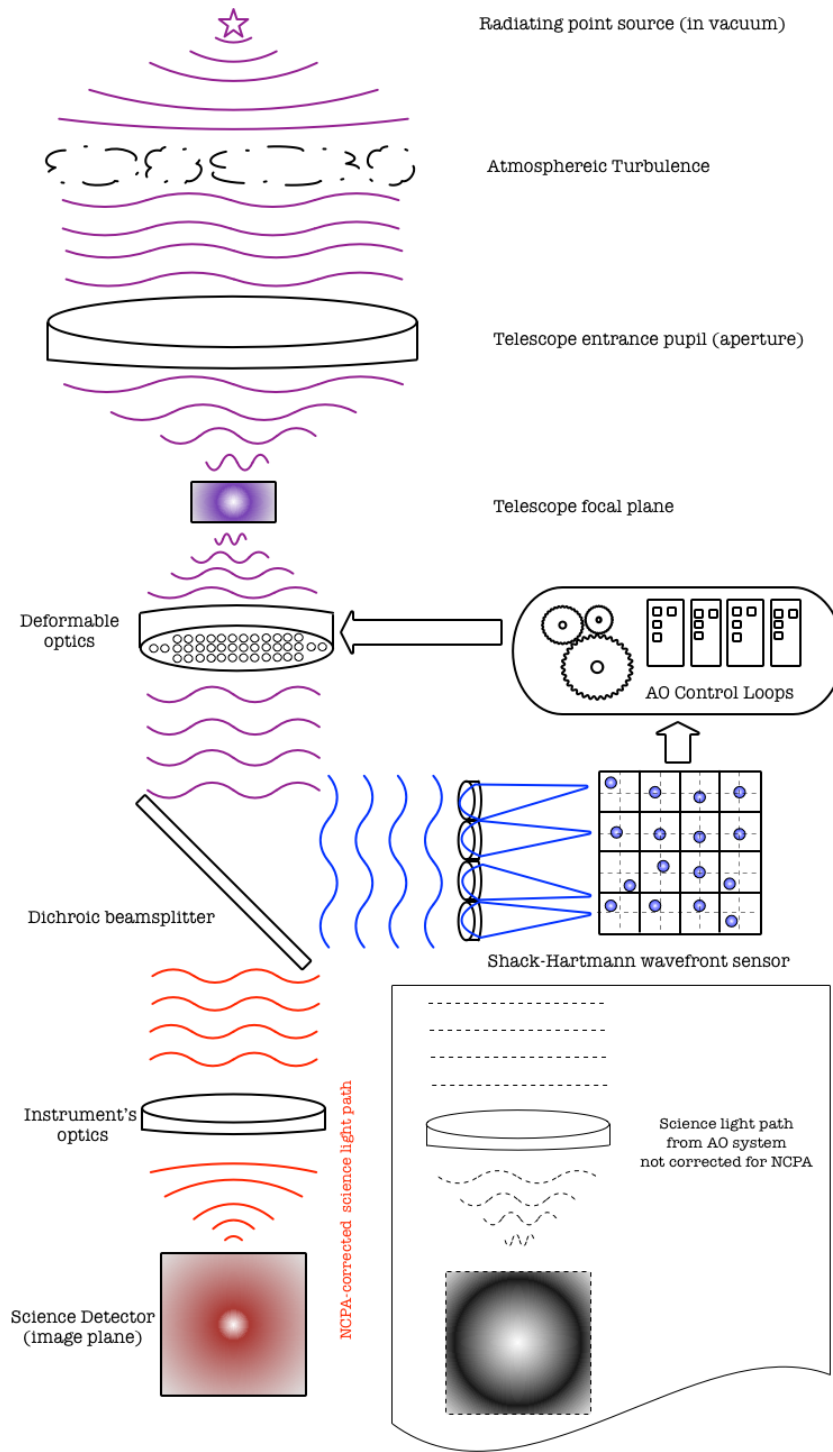
order optical and atmospheric aberrations. The primary mirror (along with the secondary and tertiary mirrors) are coated with silver so as to optimize the system for observing at wavelengths greater than 450 nm, and especially those in the infrared.

Light from the sky is reflected from the primary mirror to a 1.023m convex hyperbolic secondary mirror that is mounted on a support system with three voice-coil actuators that perform fast tip/tilt corrections and focus (the whole system is also translatable in x/y, which helps to both align the optics and correct for coma). This support system and the secondary mirror are suspended 12.5 meters above the primary by 8 10 mm-wide trusses that allow some flexibility in the case of earthquakes or other vibrational phenomenon.

From the secondary mirror, the light is then reflected back through the annulus in the primary mirror, which is baffled by a chimney, and arrives at the tertiary mirror known as the science fold. The science fold (SF) is a plane surface mirror that is mounted in the middle of the instrument support structure (ISS), a cube metal scaffold that houses instruments on either of its six sides. The SF directs the light to one of the instruments mounted on the ISS. The ISS is also attached to a cassegrain rotator that allow the field orientation to remain constant while the Alt/ Az mount tracks the telescope across the sky. The telescope delivers a beam to its instruments with an effective focal ratio of f/16, with a plate scale at the cassegrain focus of 1.61 arc seconds/ mm. On a module above the SF, there is probe that can be inserted right into the middle of the field that directs the light to Altair. After processing and correcting the wavefront, the light is then output to the science fold and on to an instrument.

While there are many more aspects to the observatory, these are the systems that will be discussed in the scope of this paper.

Altair

Altair (**ALT**ittude-conjugate **A**daptive optics for the **I**nfra**R**ed) is Gemini North's adaptive optics facility. Its uniqueness comes in the "altitude-conjugate" part, which refers to the fact that the deformable mirror is (or was originally) optically conjugate to the turbulent layer of atmosphere 6.5 km above the ground. This feature was meant to allow, at the expense of worse ground-layer turbulence correction, for a much wider isoplanatic patch and therefore a wider field of potential guide stars on any given target. Site testing during the design phase of Altair indicated that this layer was the most turbulent, and it was originally thought that the Gemini telescope's unique design of the dome enclosure and
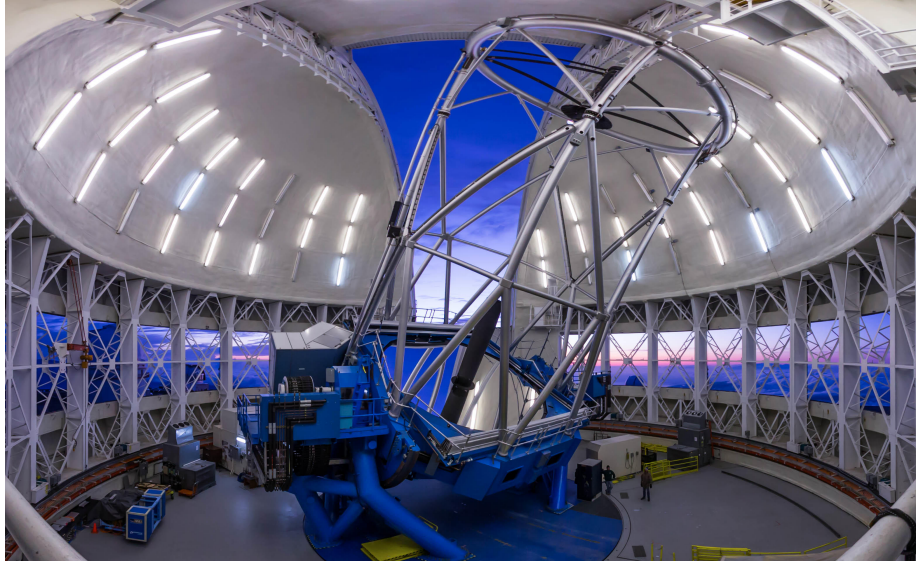
Figure 3: The Gemini North telescope facility.

other careful measures somewhat mitigate the effects of the ground-layer turbulence, and allow for this unique optical design. However, since it's construction and commissioning, it was determined that the ground layer is, indeed and by far, the most significant contributor (especially from within a dome environment, and a field lens has since been inserted to conjugate the system to the ground layer.

The deformable mirror (DM) consists of 177 actuators that can be controlled up to 1000 times per second[6] (1 kHz). There is a separate tip/ tilt mirror (TT) after the DM to take out the low-order aberrations and allow the DM more bandwidth for the higher-order corrective terms.

After the adaptive optics, a beam-splitter reflects 99% of the visible light from 400 - 850 nm through a gimbal mirror (for tracking the guide star) and a field stop onto the 12x12 Shack-Hartman wavefront sensor, while passing 97% of the near infrared light from 850 nm to 2.5 um to one of the instruments via the science fold. Everything beyond this beam splitter is considered to be in the the non-common path. Note that there is also an alternate second light path inside Altair, accessed through an moveable-stage fold mirror, that will put the

---

[6]As discussed briefly in sections 1.1 and 1.2, the actual closed-loop correction frequency is more on the order of 25 Hz when guiding light in the visible spectrum due to lag times and loop gains.
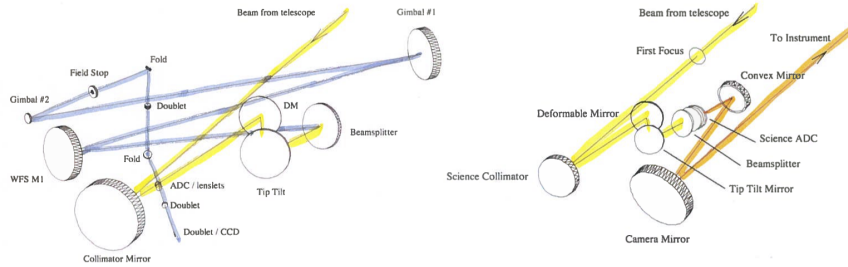
Figure 4: Altair internal optical layout. Altair WFS (blue) and Science light paths (orange) are separated by the dichroic beamsplitter. The common light paths are highlighted in yellow[11].

visible light onto three separate wavefront sensors for using a laser beacon in the sodium layer for an artificial guide star in conjunction with a fainter natural guide star for lower-order corrections (tip/ tilt) along with the differential focus of the astronomical field (science) and the sodium layer (laser WFS)[7].

Altair outputs the telescope's natural f/16 beam, and also provides a flat focal surface at the same position as the bare telescope, making it relatively "transparent" to the optical designs of the instruments.

NIRI

NIRI is Gemini North's **N**ear **I**nfra**R**ed **I**mager. Although it initially had (somewhat limited) spectroscopic capabilities as well, two key optical components (a pickoff assembly and a focal plane mask assembly) are currently non-

---

[7]While LGS corrections are not considered as part of the scope of this experiment, they are an important part of the adaptive optics suite and Gemini North and considerations for mitigation NCPA for LGS are briefly discussed in section 3.3.1
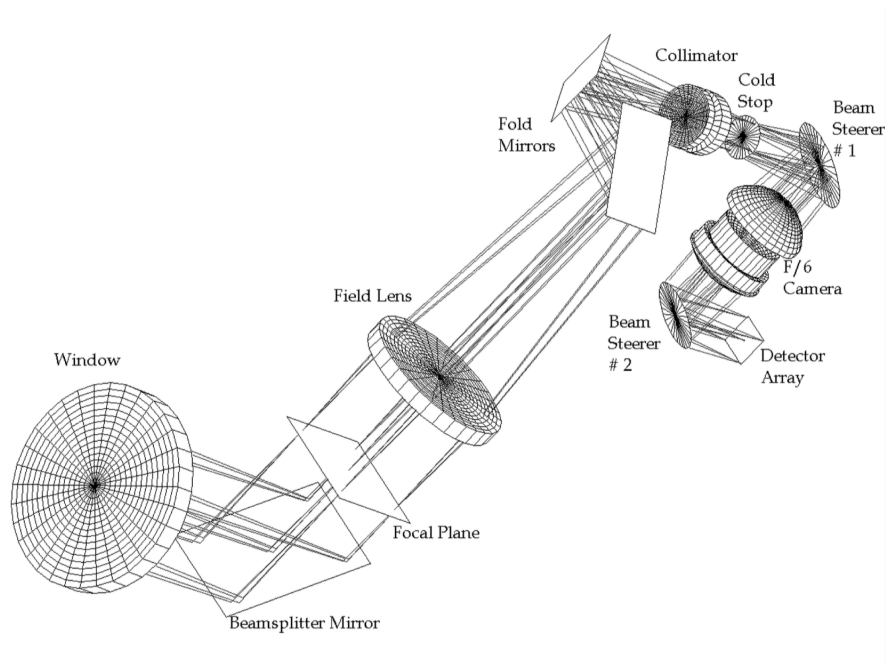
Figure 5: NIRI internal optical layout/ light path[10].

functional and therefore it is only used in its capacity as a near-infrared imager. The detector is a 1024 x 1024 ALADDIN InSb array and will image in the 1-5 micron range, which is perfect for use with Altair since Altair lets light longer than about 850 nm through. While the instrument offers three cameras – f/6, f/14, and f/32 – only the two slower cameras are used with adaptive optics. In f/14 the field of view is 51x51 arc seconds (0.05"/ pix). In f/32 its about 22 x 22 arc seconds (0.02"/pix) and therefore is very well sampled when used with Altair at near-infrared wavelengths[8]. NIRI offers a plethora of wide- and narrow-band filters covering it's entire spectrally sensitive range.

1.4.1 Image Quality Problems at Gemini North Observatory

Although Altair has been delivering exceptional imaging capabilities to its users since its commissioning over ten years ago, its performance is far from ideal, delivering only about a 15% strehl in average (~0.5") seeing conditions,

---

[8]Using the Rayleigh criterion (section 1.1) wavelengths longer than $0.8\mu m$ will be resolved. This experiment uses $2.12\mu m$ and is therefore well over-sampled.

when it should yield about 65%[1]. It is believed that there are three main underlying effects that drive the image quality problems we see today: high spatial frequency aliasing of print-through from the secondary mirror, vibrations from instruments' cryogenic cooler cold-head pumps, and non-common path aberrations. The technique of focal plane sharpening is aimed at mitigating the effects of NCPA degradation and thereby improving the image quality delivered by Altair. According to simulations, by correcting the NCPA it was estimated that up to about a 25-30% increase in strehl may be achieved.

2 Correcting the NCPA

The rest of this paper will focus on the work done to attempt to mitigate the suspected residual NCPA features. As will be presented in the following sections, the NCPA static offset was already a built-in part of the Altair control system. The intention of this experiment is to both create a more effective and efficient way to calibrate this as well as to improve the image quality delivered with Altair. Although this experiment concentrates mainly on a single camera in a single wavelength/ filter, it is expected that this work will be easily translated to other modes and instruments..

2.1 The Original Approach

Documentation concerning NCPA mitigation from Altair's commissioning (2002-2003) is unfortunately largely lacking in both content and organization, making it somewhat difficult to understand techniques and methods used in the past. In addition, most of the experts that performed the initial calibrations have since moved on from the organization, creating another obstacle in figuring out how the NCPA files were initially ascertained (among other inconveniences). However, there are various weblogs[15] and web pages[5]where somewhat scattered information can be pieced together. Most of the code used to perform the calibrations was written in IDL and still exists, so much of the effort in commencing this research was spent digging through cryptic coding and scattered web pages to piece together a picture of just how this was obtained and how best to move forward. Despite the challenges, an understanding of this work was uncovered with enough detail to both utilize pieces of it in this experiment and to determine that this technique is advantageous compared with historical

methods.

To reconstruct the wavefront after AO corrections, the use of Gemini North's High Resolution Wavefront Sensor (HRWFS) was employed. The HRWFS consists of a Shack-Harman lenslet array with 324 elements (18 x 18) and sits at the base of a fold mirror on the bottom of the ISS, at the cassegrain focus of the telescope. A star was imaged through the HRWFS at night and lateral translations of small stellar images within the sub apertures on the WFS detector were then used to reconstruct the wavefront distribution on the HRWFS. Adjustments to the NCPA file in the control loops were then made based on these measurements to effectively flatten the phase on the HRWFS.

This comparison gave an idea of non-common path effects between Altair and the telescope in general, as all instruments that are used with Altair share the optical path from Altair's BS up to the SF. While this technique is fine to get a rough estimate, it lacks accuracy in three discernible manners: it does not take into account the instruments' light paths, it does takes into account the HRWFS light path (which is necessarily different from that of the instruments), and it adds elements of relative flexure and rotation since the calibration is taken while tracking a star on the night sky[9]. Furthermore, it uses valuable[10] time on the night sky that could be used for observing science targets. These inaccuracies and inefficiencies drive the need for a more accurate and more efficient method to compensate for the static NCPA. To work around the issue of the differences in OPD (and hence "induced" NCPA), it appears that corrections were somehow introduced to the default NCPA file, although it is unknown how this was ascertained, and it is entirely possible (and it is rumored to be so) that this was a "manual" or "by eye" intervention approach. Although somewhat crude, this would be one "manual" manner in which to execute a focal plane sharpening technique.

Figure 6 shows the PSF of the calibration source imaged, with loops closed, though NIRI's f/32 camera and K-prime filter. The image on the left is taken with no NCPA correction, and shows notable astigmatism. The image on the right is taken with the "telescope" NCPA derived through the HRWFS as described above, and shows notable coma, demonstrating that the technique of determining the NCPA corrections on-sky with the HRWFS is not sufficient

---

[9]Altair's correction loops do also include flexure compensation, but it is certainly better practice to isolate those effects when calibrating for other effects, whenever possible

[10]Estimates of night sky time at Gemini are rumored to be in the approximate range of \$3 per second.
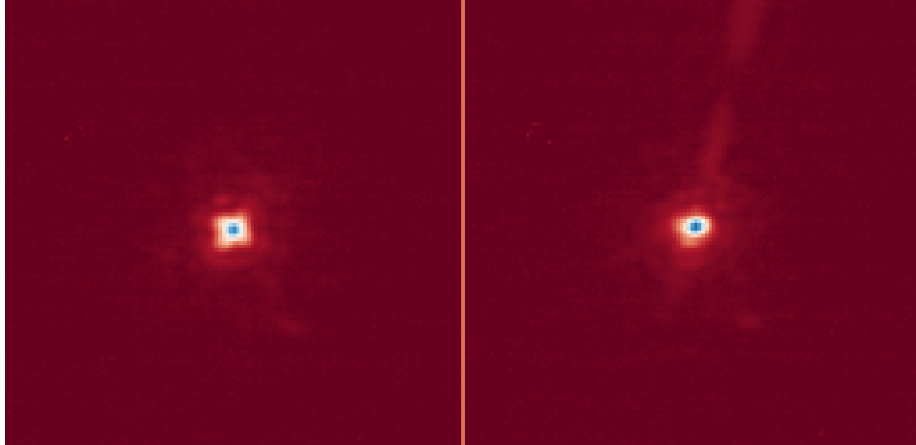
Figure 6: Examples of the PSF of the cal source imaged on NIRI (f/32, K-prime) with (left) no NCPA correction and (right) the "telescope" NCPA correction made through the HRWFS.

because it both introduces aberration from the system used and does not compensate for aberrations for other systems. Figure 14 (left, section 3.3) shows the PSF with the "default" NIRI NCPA correction (apparently derived "by eye" as discussed above) and is notably better, although does still exhibit a very small amount of 45 degree astigmatism, which is later corrected using the methods described in section 3.

2.2   Focal Plane Sharpening

Focal plane sharpening (FPS) is an empirical method of finding the NCPA by trial-and-error. The idea is to use the direct measurement of images while iterating through changes in the shape of the deformable mirror until the sharpest image is obtained. Once the state of the DM is known for the best image, the difference between this state and the nominal state will directly determine the static offset that needs to be applied to mitigate the NCPA. Since this method is empirical, there are countless ways to implement this in an experimental situation. Some considerations in choosing a method include (but are not limited to) accuracy, convergence time, practicality, ease of use, etc. The main advantage of this technique is its inherent simplicity in that results can be obtained without careful regard to the characterization of the system's properties – this is in stark contrast with other approaches, such as *phase diversity*[3], which rely

critically on the stability and precisely known system parameters.

This approach also eliminates all four of the shortcomings discussed in section 2.1 as well as offering even further advantages. Using a calibration source (rather than a star) allows the calibrations to be carried out during the day so that valuable time at night can be used more productively on scientific observations. The calibrations are run while the telescope is stationary at the zenith, eliminating any dynamic and differential flexure contributions that would otherwise be caused by gravitational forces due to the elevation angle of the telescope as it tracks across the sky. Furthermore, since the calibration source is mounted inside Altair, it is decoupled from potential rotational effects that the field might otherwise contribute. Additionally, since the vibrational problems discussed in section 1.4.1 manifest most intensely at the primary mirror (m1) and the print-through/ aliasing effects originate in the secondary (m2), which are both before the calibration source, these two major contributions to the degradation of image quality are also decoupled from the NCPA correction inadequacies. Finally, the problem associated with introducing unrelated NCPA corrections from distinctly different optics (namely, the HRWFS) is eliminated by measuring the image quality directly on the detector of the instrument being optimized. This ensures that the calibration obtained is purely related to the NCPA corrections for that specific instrument configuration.

Two main parameters must be selected in developing any algorithm that will converge on a "best" solution for the NCPA correction: parameter space and IQ metric. After selecting appropriate parameters, simulations are carried out using different algorithms before actually implementing a procedure on the systems.

2.2.1   Parameter Space

Two potential parameters, among others, for adjustments to the DM shape include Zernike modes and actuators modes.

Although there are countless numbers of orthogonal bases over which could be chosen, the Zernike polynomials offer a natural approach across a circular pupil and are readily integrated into current software and analysis scripts[11].

---

[11] Altair's DM actually uses an "Orthonormal mirror Zernike basis" which is a projection of the Zernike polynomials onto the deformable mirror that takes into account the central obscuration (pinhole mirror) and the actuators and represents very well the first 12 radial orders (up to Z136) of the Zernike polynomials[18]. For the purposes of this paper, the term

By choosing an orthonormal basis we mitigate cross-talk between terms and ensure that optimization of a single term can only increase the image quality, thereby allowing for optimization in stages. When each term can be optimized independently, obtaining precious telescope time becomes much more practical since much smaller contiguous time periods are needed, and independent results may be pieced together depending on the algorithm used.

In contrast, varying actuators on the DM individually is another intriguing potential parameter space to consider, and offers a natural approach across the actual manufactured DM since these are the finest movements that can be made. One potential advantage that this parameter may offer over using an orthonormal polynomial basis is that it could much more quickly converge on corrections of aberrations that exhibit very high spatial frequencies. In a polynomial basis, these types of aberrations may not be corrected in the first handful of terms and could therefore either remain uncorrected or take an impractical amount of iterations to converge on an appropriate solution. Furthermore, this method could mitigate problems that may be caused by performance variance across the actuators. For example, if there were an actuator that weren't functioning at its full stroke or if it weren't functioning at all, then using a polynomial orthonormal basis would never converge on an appropriate solution since the corrections themselves would be inherently flawed. However, varying individual actuators could work around this by having adjacent or even opposing actuators compensate, since this basis is inherently *not* orthonormal with respect to the phase.

In researching past techniques used to mitigate NCPAs between Altair and NIRI[5], evidence of IDL code for both types of these approaches was found, although it was not apparent that the actuator space method was ever successfully implemented.

2.2.2   Image Quality

The metric used for the solution is also quite important in influencing the effectiveness of the technique. Since FPS is an empirical method, the accuracy to which the correct offset to the "flattened" DM can be determine depends directly on how accurately the image quality (IQ) on the detector can be measured. Some potentially useful metrics include peak intensity, full width at half maximum,

---

"Zernike," when used to refer to the corrections applied to the DM, refers to this basis and not to the true Zernike polynomial.

encircled energy, Strehl ratio, noise equivalent area, and countless more.

Peak intensity might be the most straightforward way to measure the image quality, but it does not come without its disadvantages. For example, asymmetric (or "coma-like") aberrations may get improperly accounted (e.g., if for instance there were a lot of coma, but the peak of the spot was very bright despite the offset aberration in the shape). Asymmetric aberrations could also have negative effects on FWHM measurements, depending on the axis through which the cut(s) is(are) made. Of course, encircled energy would have similar limitations as well. Another interesting metric to explore might be the so-called "Strehl width," which involves comparing the image's width to the width of a uniformly illuminated disk with the same total flux and central intensity (akin to using enclosed energy)[2].

Using the Strehl ratio is a good way to avoid issues with the shape of the PSF, since it directly compares the measured peak centroid intensity with the unaberrated, diffraction limited PSF's peak at the center and therefore won't get tripped up by asymmetric aberrations or any other anomalous shape in the PSF that may fool other more simple IQ metrics. Strehl is an accepted and widely used metric in the adaptive optics community as well, so it seems like a naturally sound choice. Using Strehl ratio also makes development simpler, considering that much of the existing image analysis code in the Altair and NIRI libraries use this metric as well. Using the Strehl ratio is not without its own limitations, of course. The PSF must be diffraction limited and the background must be well characterized, or results will be inconsistent. Furthermore, the Strehl ratio must be relatively significant in order to be accurate, so a good initial shape of the DM must be known, and deviations from this shape must not be extreme.

2.3   Algorithm Selection and Simulations

Selection of an algorithm that explores the parameter space in terms of the image quality metric is also a key decision in executing the FPS technique. Studies in the field of maximization can get quite complex, and practical considerations must be taken in order to avoid negating the some of the advantages of using the technique. For the the investigations carried out in this work, two simple algorithms were considered, simulated, and implemented: the well-known downhill simplex minimization algorithm and a simple "step-through" approach.

2.3.1 Simplex Method

The goal of whichever algorithm is chosen is to maximize the IQ metric as a function of the parameter space. One well-known method of minimizing a function[12] in terms of multi-dimensional parameters is called the downhill simplex method (also known as the "amoeba" function). If the parameter space contains N dimensions (independent variables), the simplex is a "shape" with $N + 1$ points, all connected by straight lines (e.g. a triangle in two-dimensional space). This simplex shape converges on a minimum (although not necessarily a global minimum) by starting in some given configuration and moving one of its extreme points (either a maximum or minimum) through a reflection, expansion, contraction, or combination thereof until it converges to a given fractional tolerance. The concept is simplest to imagine in two or three dimensions, but is applicable in any number. It is not usually the most efficient way in terms of number of iterations to converge on a minimum, but it works well without having to perform complicated gradients or other computationally intensive operations as it only has to evaluate a given function at each iterative step[4]. Within IDL, the routine that executes this algorithm is known as "amoeba" and it takes a function with one input variable (in this case, a vector of Zernike coefficients) and morphs through the variable transformations and executes the function one step at a time. The fractional tolerance desired for convergence is entered, along with the maximum spread, or scale, of the variables and some given starting point.

Simulation

To simulate the experiment using the simplex method, a randomized phase was generated as a starting point. This was generated by adding phase contributions from Zernike terms through z22, each successive coefficient with monotonically smaller weight and such that the overall PSF held somewhat similar properties to that of the image of the calibration source through Altair and NIRI under closed loop using no NCPA correction file (i.e., about 45% strehl, exhibiting some notable astigmatisms, as in figure 6 (left)).

Zernike polynomials out to a chosen term, j[13], were generated over a circular

---

[12]Minimization and maximization are different only in semantics in that minimization algorithms can be applied to the negative of an outcome in order to maximize the function.

[13]For all purposes in this paper, the indices of the Zernike polynomials are referred to using the so-called "Noll sequential indices," or j such that Z1 is piston, Z2 and Z3 are tip and tilt, Z4 is focus, Z5 is primary 45 deg astigmatism, etc. [20]
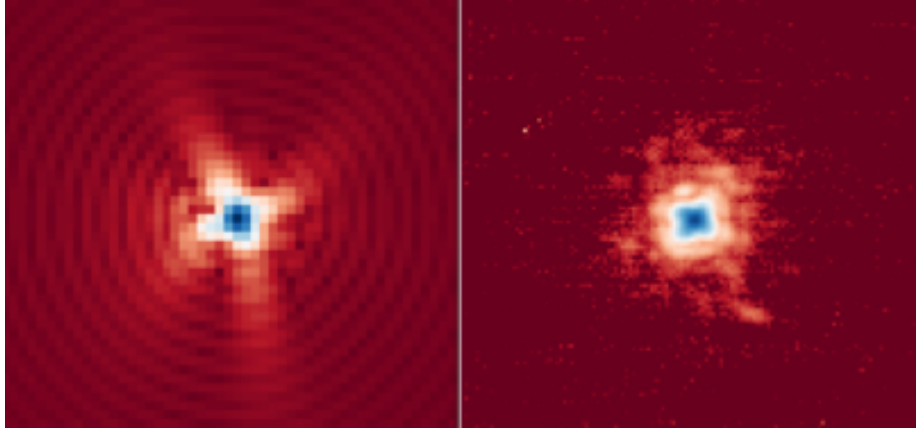
Figure 7: Comparison of initial PSF generated by simulation code (left) to that of the calibration source imaged through Altair onto NIRI at f/32 in K-prime with no NCPA correction (right).

disk to form a basis for the simulated phase. To construct the starting point, or initial aberrated PSF, coefficients for Zernike terms out to z22 (secondary spherical aberration) were generated randomly using IDL's "randomn" routine, and modified to decrease monotonically by dividing by a vector of monotonically increasing integers created by the "findgen" routine in IDL. This effectively gives a random vector where each term decreases monotonically. To mimic the typical PSF of the A-star seen with no NCPA correction in NIRI, the "findgen" factor was taken to the power of 3/4, the randomly generated vector was multiplied by two, and the two primary astigmatism coefficients were given extra weight by a factor of 3.5. When this vector of randomly generated coefficients was multiplied by the vector of Zernike polynomials, and the phase contribution from each term was summed, it consistently produced a PSF similar to[14] that seen in the images of the Altair calibration source without NCPA correction (see Figure 7), and yielded a similar Strehl ratio between 0.4 and 0.5.

In order to simulate the NCPA correction using a downhill simplex method, the phase that gave this initial PSF was then corrected by adding a phase consisting of set of Zernike coefficients through z11 that varied according to the "amoeba" function in idl (i.e., the downhill simplex routine). This technique effectively simulates moving the DM in Zernike space. The input function for

---

[14]While the central core of the PSFs of figure 7 are indeed similar, it is worthwhile to note that the outer structure (i.e., the airy rings, or higher spatial frequency portions) are not at all similar. This phenomenon will be one of the main discussion points in section 3.3.

the amoeba routine, "func," returned the negative of the Strehl value of a PSF generated by the amoeba function's variation in the coefficients. The PSF was calculated by taking the inverse Fourier transform of the absolute square of the pupil function, which consists of the complex vector $e^{i\phi}$, across the pupil[15], where ϕ is the phase generated by the sum of the Zernike polynomials and their respective coefficients. A "theoretical" PSF was generated the same way, but with no additional phase introduced. The Strehl ratio is then the ratio of the normalized maximum PSF at its center to the normalized maximum theoretical PSF at its center. Thus the "amoeba" function was given an initial (aberrated) phase and a vector of Zernike coefficients (starting with all zeros) and output a negative strehl ratio, minimized using the downhill simplex method. A functional tolerance of .001 was given to the Strehl. A weighted vector of ranges which again became weaker with successive terms was applied to the coefficients so as not to stray too far from the original, decent image quality and ensure it doesn't fall in a local minimum. Strehl ratios on the order of 90-95% were obtained using this method, and convergence times of around 60 -120 seconds were typical.

2.3.2 Step-through Method

Since the Zernike polynomial consists of independent, orthonormal terms, a "step-through" or "focusing" method may suffice as well. In this approach, each coefficient (starting at z5, 45° astigmatism) is varied and optimized by independently stepping through a range of values and analyzing each outcome to find a best Strehl ratio and its corresponding coefficient(s). Terms z1 - z4 are omitted, as they represent piston, defocus, tip, and tilt and do not distort the shape of the PSF in the same manner as the other terms (i.e., tip/ tilt are lateral displacements and defocus is a symmetric blurring, all of which are taken into account by m2, rather than Altair, on the telescope).

It should also be noted that the step-through method, if proven to work, has another very fundamental advantage: the optimization can be done piecewise in small increments (one term at a time), rather than one single run to optimize all coefficients. Obtaining access to the telescope, even in daytime hours, is not without contention and difficulty. There are always daytime maintenance tasks and other tests to be run on other instruments, etc. So having an algorithm

---

[15]A uniform apodization function was used for the pupil function: 1 inside the aperture and 0 outside.
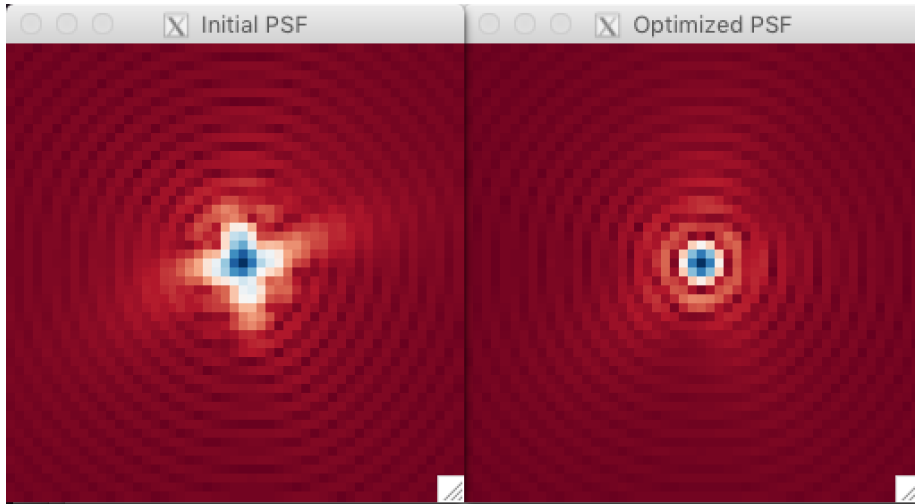
Figure 8: Simulated PSFs. (Left) Initial PSF with similar properties as we see in the calibration source through the optics with no NCPA correction; Strehl ~ 0.45. (Right) final PSF after the simplex algorithm corrected terms through z11; Strehl ~ 0.97.

that can be executed piecewise exhibits a real and practical advantage.

Simulation

Simulations were also run on the step-through method. The same phase initialization algorithm was used as in the downhill simplex method. This time, however, the coefficients were varied linearly through their selected range and the Strehl ratio was measured on each step, again calculated as described in the simplex simulation. In the simulations[16], the step sizes were incrementally made finer around the values where the maximum Strehl was found at each coefficient until a functional tolerance of 0.001 Strehl was met. The results of these simulations were indiscernible from those of the simplex method (figure 8), and yielded a Strehl of over 95% when correcting out to z11.

Again, the initial phase was generated out to z22; the purpose in not correcting all the terms was to provide a conservative buffer for a real-world scenario where there may be higher-order effects than we can realistically account for. When corrected to z22, Strehl ratios of over 0.99 were obtained in both methods,

---

[16]In the actual experiment a parabolic fit was found to be just as useful as incrementally tuning the step size, due to the standard deviation of the measurements (i.e., the Strehl was only determined to within .02, and the coefficients to within .01 μm, and thus using a polynomial fit saved a extreme amount of time).

and served as a sanity check that the programing was functioning as designed and expected.

2.3.3 Other Methods

The algorithms highlighted in this paper are of the very simplest sort, and it is worth mentioning that attempting other minimization techniques, such as Powell's method or even a much more complicated approach such as the Ferret algorithm suggested in [3], may be more efficient and effective. Approaches such as these, and even exploring the simplex method further, may rely on the observatory's prioritization of obtaining more reliable detector control electronics, as they certainly demand that many images be taken successively See section 3.2.1 for a brief discussion on the instrument instabilities that impede such methods at Gemini North. That being said, the maximization and minimization algorithms could also be adapted to not be so susceptible to electronics crashes, and be edited such that they could pick up where they left off.

3 Experimental Results and Discussion

This section will describe the design and experimental set-up, the data collected and their analysis, and a discussion of the results and their meaning and significance in terms of improving the image quality delivered through Altair at Gemini North.

3.1 Experimental Design

The experimental configuration and design and the data collection processes are presented in this section. The flowchart presented in figure 9 below shows the generalized approach to the design of the experiment. The initializations, which include the alignment and verification procedures, are done first and the automated procedure that was developed for this experiment follows: an image is taken, the image is analyzed to obtain the Strehl ratio, a new NCPA adjustment is made and implemented, and this process continues until the maximization is reached according to the criteria set.
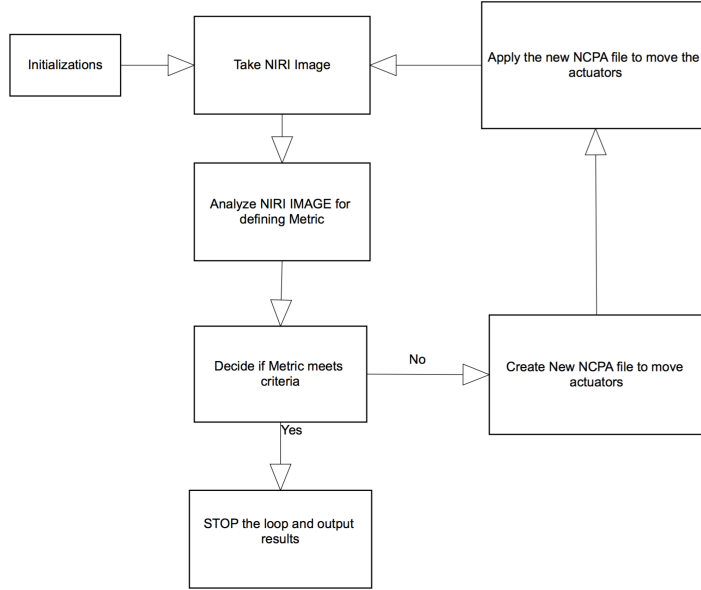
Figure 9: Flow Chart for generic FPS algorithm (same concept is used for both simplex and step-through methods).

3.1.1 Initializations and configurations

While the majority of the data collection was taken autonomously after software code was developed, each session had to be manually configured as described below.

The telescope was moved to the zenith position and locked, and the cassegrain rotator was left parked at a random location in each session (since the field is internal, there is no rotational dependence). Altair's control matrix, which sets gain parameters derived from environmental data such as wind speed, r_0, seeing, etc., was set to its default, as is practice when doing work with the calibration source.

A pinhole calibration source (known as the "A-star", or *artificial star*) was inserted near the entrance of Altair, replacing the field lens near the telescope's focal plan. Altair was configured in "NGS mode" such that light from the source travels through the NGS light path and is imaged onto the NGS WFS for closed-loop correction. Guide loops were then closed and the A-star was imaged on

the NIRI detector through the K-prime filter and the f/32 camera where its position on the detector was ascertained. Loops were then opened and the A-star was translated towards the center of the NIRI detector. The calibration source was then aligned by eye on the WFS by means of a movable gimbal mirror (see Figure 4) as the WFS was read out in real time and light was distributed evenly across its sub-apertures[17]. This process was iterated manually until the A-star was near the center of the NIRI detector, avoiding any bad pixel patches, and also aligned on the NGS WFS. Since the positions of the steering optics and/ or the A-star were not repeatable to a reasonable enough accuracy, this procedure was done at the beginning of each session. The repeatability issues may stem from daily calibration (and hence movement) of the Altair steering gimbal mirrors, or may lie in the A-star/ field lens assembly mechanism, which is also a part of the daily calibration procedures.

The NIRI configuration (f/32 camera at $2.12\mu m$) was manually implemented using the instrument's EPICS dm-screen interface, and was chosen for this experiment for two reasons. First and foremost, it is oversampled (see section) and therefore the diffraction pattern should be easily discernible, and calculation of the Strehl ratio should therefore be accurate. Secondly, the nightly instrument monitoring program known at Gemini as "SV-101" is set up in the same configuration to image a bright star at the beginning of each night, so there is a huge amount of data for easy comparison, especially for when the results are implemented on-sky. The exposure time was set at 0.05s x 20 co-adds for a 1s total integration time. In order to test the configuration, the last image taken after the alignment was analyzed to extract a radial profile in PyRAF software so that it could be checked for saturation and other potentially adverse effects. Images are stored in the FITS format, which also contains header information about the parameters discussed above. They are stored in the Gemini Archive, and a copy of each was also moved to another personal permanent directory for ease of access.

3.1.2 Coding the Algorithm(s)

IDL code was developed for this experiment that is analogous to the algorithms described in the sections about the simplex and step-through simulations in section 2.3. For this development, as stated earlier, some of the more techni-

---

[17]Note that this "eyeball" alignment is just fine since the internal TT mirror, when the guide loops are closed, will correct for any small misalignment.

cal coding was already available in the form of IDL functions and procedures[18], and this code was studied and incorporated into the algorithms designed for this particular experiment as described below.

The "func" Procedure

A function named "func" was developed as the "heart" of the code and covers the top three blocks in the flowchart in figure 9: applying corrections, taking the image, and analyzing the image. The reason for the naming of the function was simply that the "amoeba" procedure in IDL expects this name as the function it calls to work with in its minimization. "Amoeba" furthermore expects only one input variable. For this experiment the variable, c, was the vector of Zernike coefficients, and all other variables that passed between procedures and functions had to be inserted into a common block of variables rather than be defined as a parameter of the function. A detailed description of the function "func" follows, and the code itself can bee seen in Appendix C.1.

The first thing that "func" does is open the guide loops (if they're closed) and update the NCPA file. Loops are opened with a simple I/O routine from the Gemini IDL library that was modified slightly for this project. With the loops open, the NCPA file is adjusted with the addition of a vector of Zernike coefficients – this vector will be addressed in the following paragraphs and is defined by other procedures in the algorithm. A Gemini IDL procedure named "updateAoNcpaPar" handles converting the Zernike coefficients into the NCPA matrix that sets the static offset on the actuators. The output of this procedure is a new NCPA file, which can then be set as the new default offset using an IDL function developed for this project named "setncpa." Note that the first iteration of "func" (depending on the procedure that calls it) usually calls a vector of zeros to the "updateAoNcpaPar" procedure and hence the NCPA offset is not actually changed until the second iteration. Each time the NCPA file is loaded, a control matrix has to be initialized, so a simple script called "clickCreateNewControlMatrix" was developed that simply loads the default control matrix as discussed above. The NCPA files themselves consist of a large and complicated matrix that is added to the reconstruction term as a static offset in actuator voltages that correspond to a "zero point" in the spot positions on the WFS (i.e, a_{NCPA} from section 1.3). This is the file that is updated by the

---

[18]Although some code already existed, documentation was rare and unclear, and a good portion of the work on this project went into studying the old code to figure out how to hook it into these relatively simple algorithms.

outcome of the experiment, and there are two such files for each instrument that is used with Altair (one for LGS and one for NGS – this project focuses on the NGS calibration).

After the NCPA file is updated and loaded, the guide loops are closed again and a wait-time of 16 seconds is begun in order to let the loop gains and corrections settle. The value for this wait-time was adopted from historical implementations of NCPA corrections as discussed in section 2.1 and should be more than sufficient for a calibration source, since it was originally used on a stellar source which needed time to calculate seeing measurements and bandwidth to adjust tip-tilt according to local seeing variability and wind speed, etc. Between the end of this wait period and image integration, a quick check was implemented to make sure the loops were still closed and correcting due to some instabilities in the optimizer whereby the reconstructor would lag and loops would spontaneously open. Although this was a relatively infrequent occurrence, it transpired enough (and during a period of time when the experiment was unattended) to warrant the development of this extra automated check. If the reconstructor was found to be lagging, the loops were simply commanded to re-closed and another 16s wait-time commenced.

When the 16s wait-time and reconstructor check is done, a series of images is taken on NIRI and each one is analyzed individually. The number of images taken is usually set during the initializations which take place in a separate procedure, but can be set in "func" if no such parameter is included in the common variable block. Due to the variability in background noise and in Strehl measurements, this number was nominally set to 10 in order to provide a good sample over which to average. The procedure "goniri" was developed to simply tell the detector controller to take an image; all other parameters, such as integration time, filter, instrument configuration, etc., are set manually in the initialization stage described above. After one image is read out, the file is converted to a two dimensional array in IDL using a procedure called "fits_read" from the IDL Astronomy User's Library. The "sky" image (taken as an initialization in whichever procedure calls on "func") is then subtracted from the image to remove bad/ hot pixels and give the image a zero-baseline. A function called "histmax" is then called to calculate the *mode* of the histogram which is used as a background measurement for the Strehl calculation[19]. The

---

[19]The "fwhmstrehl" routine actually does its own automated background estimation using interpolation of the zero-point in the MTF, but the histogram background was both found to be very accurate and to provide a good check against the automatic background calculation

```
Image Number | Measured Strehl Ratio | Zernike Coefficients (a)
------------   ---------------------   ------------------------
     1414.00      0.503647    -0.114133      0.0396231     -0.0227607       0.159316      0.058750
     1415.00      0.482196    -0.114133      0.0396231     -0.0227607       0.159316      0.058750
     1416.00      0.493930    -0.114133      0.0396231     -0.0227607       0.159316      0.058750
     1417.00      0.514152    -0.114133      0.0396231     -0.0227607       0.159316      0.058750
     1418.00      0.526502    -0.114133      0.0396231     -0.0227607       0.159316      0.058750
     1419.00      0.487346    -0.114133      0.0396231     -0.0227607       0.159316      0.058750
     1420.00      0.492145    -0.114133      0.0396231     -0.0227607       0.159316      0.058750
     1421.00      0.523362    -0.114133      0.0396231     -0.0227607       0.159316      0.058750
     1422.00      0.477534    -0.114133      0.0396231     -0.0227607       0.159316      0.058750
     1423.00      0.446237    -0.114133      0.0396231     -0.0227607       0.159316      0.058750
Mean Strehl with these Zernike coefficients is S~       0.494705     +/-     0.0239263
```

Figure 10: Example log file from the output of "func," and IDL routine developed to automate the setting of NCPA file, taking of image with NIRI, and analysis of that image.

Strehl ratio is then calculated in a function called "fwhmstrehl," which is also a part of the Gemini IDL library. It calculates the Strehl ratio by comparing the maximum intensity of the image's PSF, normalized by its total intensity to the maximum of the theoretical PSF (or airy pattern) given the OTF of the system, normalized by its total intensity. Then, for each image in the series, the "func" routine stores the Strehl value in an array and after the last image the mean value and standard deviation are calculated. Note that on each image, the "func" routine writes a log entry with data about the calculated Strehl, the Zernike coefficient values, and the corresponding image name for reference. A line with the mean Strehl and standard deviation is also included at the end of the output of the log file. Figure 10 shows an example of such a log file. The result of "func" is the *negative*[20] of the calculated mean Strehl ratio.

The "NcpaSimplex" Procedure

Another IDL procedure called "NcpaSimplex" was developed to fulfill the roles of the other four blocks in the flowchart (figure 9): initializations, creation of NCPA offset vector, and criteria decision-making. This procedure first initializes parameters and log files that are used in the "func" routine, then it uses a well-known minimization algorithm to vary the Zernike coefficients (via the "func" function described above) and decide if/ when the tolerance criteria is met. This code is included in Appendix C.2.

To initialize Altair, the procedure loads all NCPA default files (including the NIRI, GMOS, "zero," "telescope," and "test" files) to the temporary IDL

---

in the "fwhmstrehl" procedure.

[20]Again, this is because the "amoeba" routine *minimizes* its input function.

directory, and the user is prompted to select one to start. The default NIRI file was the usual starting point for the simplex routine[21], as it provides a decent initial Strehl ratio in order to help avoid falling victim to local minima. After selecting a NCPA default state, the wavelength, number of corrected terms, number of images on each iteration, any pre-determined coefficient offsets to the default file, the scale over which to vary the coefficients, and the fractional tolerance are all set. All log files and arrays for this procedure and for "func" are initialized here as well.

The next initialization performed is taking a "sky" image. Throughout the beginning stages of testing, a sky frame was not used, and there were, from time to time, problems with consistency in Strehl measurement and with hot/ noisy, or dead pixels. The code was later revised to take the sky frame by turning off the A-star, taking a NIRI image, reading the file into an IDL matrix, and saving it to the block of common variables such that it can be picked up by "func."

After the initializations, the creation of offset coefficient vectors and making decisions as to whether the criteria was met was left to IDL's built in function, "amoeba." As mentioned in section 2.3, the "amoeba" function uses the down-hill simplex routine as described in [4]. This well-known and simple, yet very effective and relatively fast minimization algorithm makes a shape of $N+1$ sides (where N is the number of arguments in the input vector), usually starting at an extreme end of the scale provided) that stretches and folds its way to the minimum value of the input function. In this case, the function is "func" and the output is the negative Strehl ratio. The input vector is a, the Zernike coefficients up to the highest term being corrected. For this experiment, the starting point was a vector of zeros and the fractional tolerance was varied during the countless trials of executing this algorithm.

The end result of the simplex algorithm, in principle, is a maximized Strehl ratio and its accompanying Zernike coefficients. In practice, the limitations of the detector controller electronics inhibited the algorithm's success (and practicality) significantly. See section 3.2.1 for a detailed discussion on the hardships presented by the hardware.

The "ncpastep" Procedure

---

[21]During the simplex testing stages, handling for the "test" file was not yet written and was therefore unavailable. Besides, the "amoeba" function is an "all-or-nothing" routine in that it needs to settle on its minimum or it doesn't exit cleanly (although there are still log files from which to recover data).

The procedure written to execute the "step-through" technique was named "ncpastep." This procedure fulfilled the same parts of the design flowchart and used many of the same initialization procedures as the "NcpaSimplex" code discussed above, including setting initial parameters and taking a sky frame, etc. The code in its entirety can be seen in Appendix C.3.

One difference is that this procedure was aimed to alleviate the need to complete the optimization of every term simultaneously, so it was designed to do one coefficient per run. Therefore, the initial parameters also included setting which term to correct (i.e., z=5 for primary 45-deg astigmatism, z=6 for primary 0-deg astigmatism, etc.), and the selection of the number of steps with which to walk through the coefficient variations (and hence by how much to vary them on each step). Also, after the first few terms in the polynomial, it becomes cumbersome to enter the coefficients manually on each run, so a method to save the output to a temporary or "test" NCPA file was devised and henceforth used instead of reverting to the default NIRI file on each trial.

Coding the actual procedure was relatively straightforward. The number of steps were input along with the range over which to vary the coefficient, and this information gives step sizes and hence the values of the vector to input to the "func" procedure (i.e., divide the range by the number of steps to get the interval, start at the negative range and step through accordingly – note that a "0" value is always added and the value of the range on both the positive and negative sides are anchored). Using the "test" NCPA file as a default input (assuming the test file has the first n Zernike coefficients already maximized), the vector, a, input to the "func" procedure to maximize the $n + 1$ coefficient is simply a vector of $n + 1$ zeros. Of course, the option to manually define the coefficients is always available as well. Once the output of "func" was recorded and logged for each step in the range of the coefficient, a plot of Strehl vs. coefficient value was generated and a second-order polynomial fit was produced with IDL's built-in "poly_fit" routine. Then the coefficient that corresponds to the maximum value is simply where the derivative is zero (e.g., $x_{max} = \frac{-b}{2a}$). This value is then input to the "updateAoNcpaPar" in order to be converted to the appropriate addition in the NCPA file and saved as the new "test" file. This process is iterated as far as it is warranted, and can be done on individual terms in separate sessions, which not only eludes hardware issues related to length of use or number of images taken, but also allows the procedure to be done just about any time the telescope is free for 30 min or more throughout the day, whereas the simplex routine took many hours without convergence before its

failures.

These three IDL procedures make up the bulk of the engine that drives the experimental design through the different steps of the process outlined in the flowchart (figure 9). The "func" procedure takes care of taking and analyzing images, storing data in log files, and applying corrections to the NCPA files, while either the "ncpastep" or "NcpaSimplex" procedures take care of initializations and decide how and when to vary the NCPA files, according to the two different algorithms discussed. While proving useful for this experiment, it should also be noted that this code will undergo some refinement in the near future and be made available to all of Gemini; it lays some significant groundwork for future tests, procedures, and experiments.

3.2   Results

In the following section, the results of implementing the above algorithms are presented as well as a discussion of the meaning of the outcome(s) and upcoming future related work.

3.2.1   Simplex Routine

For the Simplex Routine, the "NcpaSimplex" code described above was used to execute the experiment after the manual alignment and calibrations were completed. Fractional tolerances up to .02 in Strehl[22] were attempted, as well as many variations of the number of coefficients to correct, from 2 to 18. Ranges on the coefficients from .2 to 1.0 μm were also investigated as the experiment progressed.

Unfortunately, this routine ran into problems with the stability of the detector controller, and an acceptable convergence was never reached. The data from logs on multiple attempts to optimize the NCPA over both 2 and 8 terms using the simplex algorithm did indicate, however, that the z5 (45º primary astigmatism) term[23] was converging around -.15μm, which was consistent with

[22]There was an initial misunderstanding of the definition of "fractional tolerance" which is now understood as the allowed variation for convergence at any given simplex point (i.e., vector of Zernike coefficients), or $2 * \frac{Strehl_{max} - Strehl_{min}}{Strehl_{max} + Strehl_{min}}$. Thus the upper attempt at 0.02 would only lead to convergence, given the standard deviation of .02, if Strehl values were near the 90th percentile range. However, after this mistake was noted, the data from the logs were re-evaluated and were not seen to be converging in entirety before any of the NIRI DC crashes.

[23]End results determined that no other term up to z49 gave significant degradation to the

39
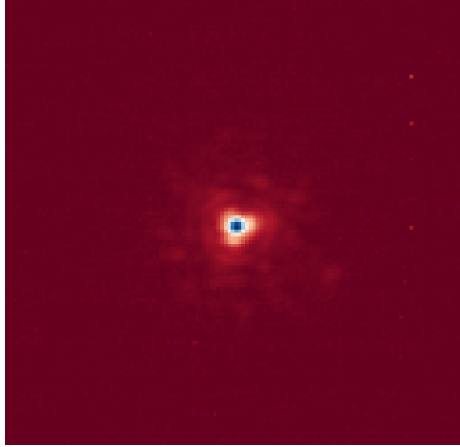
Figure 11: PSF towards the end of the longest simplex run. The Simplex routine was converging on a local minimum that exhibited a significant trefoil pattern.

results from the step-through method discussed in more detail below in section 3.2.2. That being said, the simplex routine also noticeably got "stuck" in a local minima during its longest uninterrupted run, which is a known limitation of the downhill simplex minimization algorithm: note the apparent trefoil signature in the PSF of figure 11, which is one of the better images where the simplex routine was converging.

The NIRI detector suffers a known fault on its GNAAC controller whereby every so often (seemingly correlated with the number of images taken over a given period of time) the electronics "hang" and the VME module needs to be power-cycled. Since the simplex method used here relies on a readily available but self-contained IDL function, it was not straightforward to save progress within the evaluation of the "amoeba" function, and therefore any time the NIRI detector crashed, the procedure needed to be restarted from the beginning. The more variables that needed to be corrected, the more iterations needed to be run, and the more likely the routine would not finish before the GNAAC crash/ hang was encountered. The longest simplex run before a DC crash went out to 113 iterations of "func," which means about 1130 individual, successive images. The large number of iterations needed for this routine is due to the high number of terms that need to be corrected (at least 8 to match current NCPA files). This high number of iterations needed to converge coupled with the 10

PSF, as all other coefficients were optimized at values of $< 0.03 \pm 0.01 \mu m$.

images for each iteration (to account for variance of Strehl calculations) is what drives the number of NIRI frames to levels high enough to see these detector crashes frequently. Thus, the simplex routine, as written for this experiment, was deemed impractical and results were not utilized other than as a check against the step-through method results.

3.2.2   Step-through Routine

The step-through routine was developed to avoid the nuances of the instruments involved such that data was output and saved between every step to avoid a situation similar to that encountered in the simplex routine. The control loops were fed a vector of Zernike coefficient offsets and told to modify one of them through a prescribed range and number of steps to iterate. The range was determined to be about $\pm 0.4 \mu m$ during some of the initial trials by looking at how the PSF changed with the variation of the value. With the lower-order terms, the PSF would smear as determined by eye at about $\pm 0.3 \mu m$, so using 0.4 for the range added a healthy buffer to allow for a confident fit. The number of steps, again during some initial trials, was varied between 5 and 9, but was left at 5 for the majority of the work. This was determined due to the tradeoff between the accuracy of a fit and the efficient use of time on the telescope.

Images were evaluated by the code at each of these intervals described in section 3.1.2, and the resulting mean Strehl ratios were fit with a parabola to determine the coefficient that gave the maximum Strehl ratio (Figure 12). The parabolic fit gave the three coefficients for a second-order polynomial (i.e., a, b, and c from $ax^2 + bx + c$), and setting its derivative equal to zero to get the x-value for the maximum was straightforward. The 10 Strehl ratio measurements at each step were used to obtain a mean Strehl and standard deviations which were then fed into a Monte Carlo simulation to obtain an error estimate on the coefficient value by doing this fit procedure 100,000 times on randomly generated strehl values within their respective errors at each coefficient offset. The coefficient offset relating to the maximized Strehl ratio was determined to have a standard deviation of about $\pm 0.01 \mu m$.

This value was then used as the "default" coefficient for that particular Zernike term and the next coefficient was analyzed similarly, but now with a somewhat more optimal NCPA correction applied (i.e., a better starting point). The optimal coefficients calculated were saved and could then later be re-applied whether this was the next day, week, or minute. This mitigated many technical
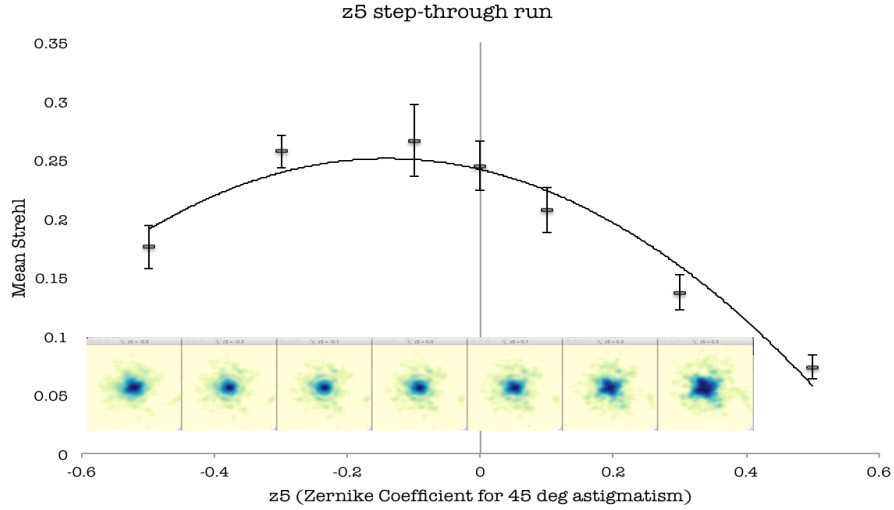
Figure 12: A parabolic fit through 7 values of Strehl vs. z5 showed a maximum at about z5 = -0.14μm (PSFs shown below plot).

and practical difficulties in carrying out the experiment.

Coefficients out to z49 were investigated using the step-through algorithm, and improvements in Strehl were noted, but painfully slowly after z5. The z5 term was significant, however, and showed about -.15 μm of residual 45$^{\text{o}}$ astigmatism; all other optimized coefficients were seen to be $\leq 0.03\mu m$ (see appendix B) .

The error in Strehl measurement on any given set of 10 images with a single NCPA file was on the order of 2%. Improvements in Strehl out to z37[24] show an increase of about 6% in strehl from our current NCPA correction, corresponding to an improvement of around 11%. The main contribution to the NCPA was the first term, z5 (45$^{\text{o}}$ astigmatism) and this can be seen by eye in the PSFs in Figure 13 below, which shows a comparison of the PSF with the default NIRI NCPA correction and the newer optimized correction.
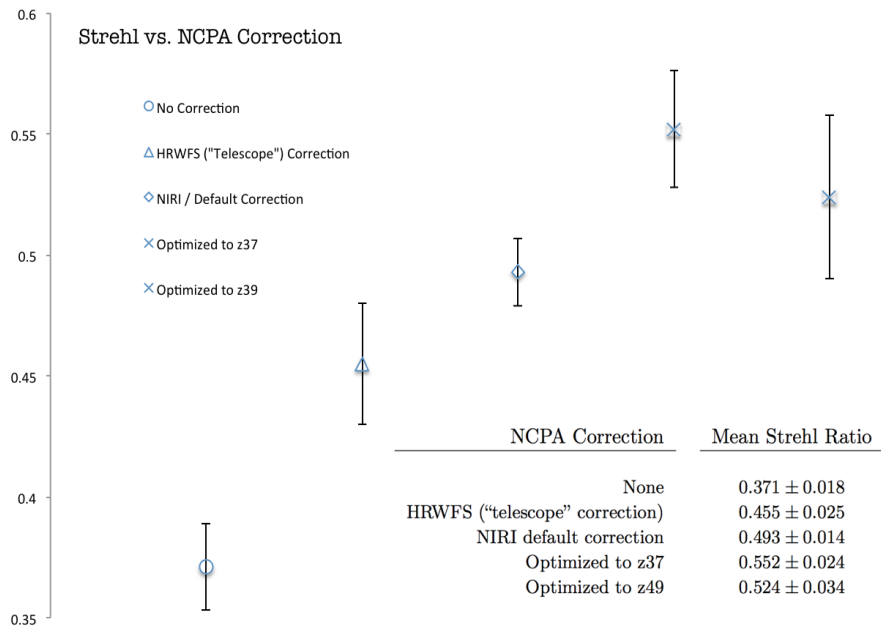
Figure 13: Strehl ratio vs. NCPA correction

The figure contains a chart titled "Strehl vs. NCPA Correction" with legend:
- No Correction
- HRWFS ("Telescope") Correction
- NIRI / Default Correction
- Optimized to z37
- Optimized to z39

NCPA Correction	Mean Strehl Ratio
None	0.371 ± 0.018
HRWFS ("telescope" correction)	0.455 ± 0.025
NIRI default correction	0.493 ± 0.014
Optimized to z37	0.552 ± 0.024
Optimized to z49	0.524 ± 0.034

3.2.3 Variation With Filter Selection

This experiment concentrated mainly in the K-prime regime, where, at $\lambda = 2.12\mu m$, the detector is oversampled and therefore it is easier to assess more subtle changes in the PSF. However, after demonstrating that the technique worked on a well-sampled PSF, astigmatism coefficients for other wavelengths were tested to determine if the filters play a significant role in NCPAs. The results of this quick test showed us that the coefficients are mostly optimized in a consistent manner at other filters[25]. Therefore obtaining several NCPA

---

[24]Note that corrections up to z49 seem to show a decrease in Strehl from corrections to z37. The data for corrections to z49 were taken on a different day and the NIRI detector was noticeably noisier than usual, which is reflected in the error bar (standard deviation). The value at z5 - z37 is within the margin of error of the mean value at z38 - z49, but the opposite is not true, which suggests that the mean value of the z38 - z49 corrections was most likely on the low side of its error budget.

[25]These were coarse measurements to quickly test whether the coefficients were "in the ball park," and the only suspect one was the FeII z6 measurement, which was slightly indicative that a very small amount of astigmatism may be introduced, but further refined measurements need to be done before anything quantitative is deduced. For all intents and purposes, the results suggest that we are "in the ball park."

	FeII (1.64μm)	H-band (1.65 μm)	J-band (1.25 μm)
Default NCPA correction	0.29 ± 0.02	0.31 ± 0.01	0.20 ± 0.01
NCPA optimized to z6	0.34 ± 0.02	0.36 ± 0.01	0.23 ± 0.02
(z5,z6) optimized offsets	$(-0.14, 0.05)$	$(-0.11, 0.01)$	$(-0.10, 0)$

Table 1: Optimizations of first two (astigmatism) Zernike polynomial terms through three other filters. The coefficient offsets are on the order of those found for the K-prime filter (mostly) within $0.03\mu m$ ($< \lambda/50$).

correction files for multiple filters may be a futile effort since it would involve many hours of effort on changing software interactions on how and when these NCPA files are loaded in Altair, and also could involve adding overhead to on-sky observations to gain a very small, if at all measurable, amount of image quality.

3.3 Discussion

This experiment, first and foremost, determined that the procedure developed is practical and works to improve image quality by mitigating non-common path aberrations. Furthermore it is an improvement over historical applied techniques. A comparison of the current NCPA file and the optimized one to both the "zero" NCPA and the "telescope" NCPA (discussed in section 2.1, Figure 6) shows that it is clear that there is both a need for the correction and that the previous method of measuring the NCPA from the HRWFS did not work as well, most likely due to the lack of accurate correction for the science path (section 2.1). This is an important part of the result in that the NCPA for other instruments and cameras can now be calibrated using this technique (after some minor refinement). The technique does not use time on the sky and it can be done in small, 30-minute intervals of time, allowing for a productive day and night of regular telescope maintenance and operation. In effect, its "cost" is virtually nothing, and expected gain is significant.

Secondly, this experiment accomplished what it set out to do in principle, although perhaps not in magnitude. Figure 14 shows a comparison of the PSF of the calibration source using the default NIRI NCPA file (left) and after correction with the new optimization done in this experiment (right). While the resulting PSF isn't drastically improved on the order of the expected 30% Strehl, it is visibly improved in that a smoother and more complete first airy ring and a more circular core and disk is seen (the left PSF exhibits a small but notable

44
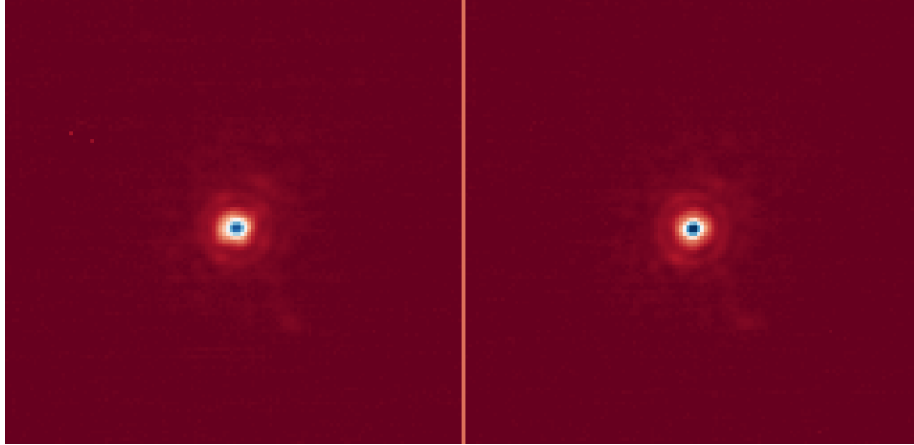
Figure 14: PSFs of the calibration source imaged in closed loops through NIRI (f/32, K-prime) with (left) the "default" NIRI NCPA file correction applied and (right) the new NCPA correction, optimized through z37.

diamond-shape from the 45º astigmatism).

Perhaps another significant outcome of this experiment is the unveiling of a previously unknown potential issue with the facility Adaptive optics system. Inspection of the PSFs in Figures 6 and 14 shows a consistent "spot" at around the 5-o'clock position and other fainter, static "speckles" that appear at and outside of the first airy ring. These are evidence of high spatial frequency structure that remains uncorrected through (or introduced by) the adaptive optics system. Even while correcting very high-order Zernike terms, up to z49, these spots were persistent and remained uncorrected and mostly unaltered[26]. When imaging a calibration source through virtually no turbulence on a well-sampled detector through an optimized adaptive optics system, Strehl ratios in the high 80 to low 90 percentiles were expected[27]. This phenomenon suggests that it will certainly be worthwhile to explore these effects and attempt to correct them, as there is likely around 30% Strehl to be gained if they can be mitigated.

---

[26]These features showed variation only when applying significant amounts of aberration ($> .25\mu m$),and not when the coefficients were optimized

[27]In previous experiments[17], it was noted that 90% Strehl values were obtained, although sporadically. While this result wasn't seen even once in hundreds (if not thousands) of measurements, the streaking and vibrational phenomena were also not seen, so it may be that some aspect of the system has changed since then. Investigation to this detail has been commenced and is ongoing.

3.3.1 Future Considerations and Improvements

The efforts furnished and products developed throughout this research lay important groundwork for upcoming projects aimed at improving the image quality delivered by Altair at Gemini North. The following section presents a discussion on some planned and suggested projects and studies for the near future.

Implement the model and test it on the sky

The first order of business is to implement this model on the sky. Engineering night tests (ENT) for on-sky verification are being planned and are expected to be executed in May of 2016. The tests will consist of taking images at f/32 in K-prime on NIRI of a bright point source while closed-loop through Altair in good and stable ($<\tilde{\ }.6$") seeing conditions with both the current and the new model at various elevation and rotation angles. These tests aim to investigate the performance of the new NCPA model. It may be that the increase in strehl is negligible beneath the other degradational features of the system, but it is expected that in good seeing a slight improvement may be seen. Current Strehl ratios[1] in moderately good seeing conditions (.6") in the K-band are measured at about 0.15, so an 6% increase in Strehl ratio would yield about 0.21. In good seeing conditions (.5" and better) Strehl ratios of around .2 are currently seen in the K-band, and improvements on the order indicated from the results of this work suggest Strehl ratios in these conditions with the optimized NCPA applied to be on the order of .26, an improvement of up to 18%.

Implement customized NCPA files for other instruments and cameras

The technique was shown to work for at least low-order, low spatial frequency degradations in the PSF'. Therefore it is prudent to immediately apply the technique to the other instruments that will use Altair for imaging: namely NIFS and GMOS, as well as the NIRI f/14 camera. All three of these instruments use (or will use) Altair to provide corrections to the turbulence for imaging celestial sources for scientific study. Implementing an individualized NCPA term to the corrective loops can only help improve the image quality provided. Currently, all instruments use the default NIRI NCPA file for NGS corrections. Software that changes this static DM offset on each telescope + instrument configuration (i.e., each time a new target is slewed to) is already implemented, and the only work

left to be done is to characterize the files associated with these modes. Work to implement this will proceed immediately and should be relatively simple to carry out: the only changes to be made are to analyze images with a non-Strehl metric (i.e., max intensity or FWHM) since the other instruments and camera are not over-sampled.

Furthermore, the NCPA corrections in LGS mode are known to "drift" over time on approximately 3-6 month time scales[5], and haven't been reassessed in quite some time (several years). Developing a daytime technique to optimize the LGS NCPA corrections, although slightly more complicated due to an off-axis calibration source for the LGS WFS, may be significantly beneficial to image quality in this mode. Similar algorithms could be developed using the LGS calibration source. Past implementations of NCPA corrections in LGS mode were similarly done on the sky using the HRWFS to measure the coefficients directly, which have been shown to give results that are not specific to the science path and therefore inaccurate.

Investigate High Spatial Frequency Structure in the PSF

As noted in the initial discussion of the results (section 3.3), this experiment uncovered a high spatial frequency structure in the PSF of the calibration source at relatively low orders in the orthonormal basis. The fact that the structure can be seen in the second (and even slightly in the first) airy ring suggests that these are not likely "edge effects" or effects due to polishing errors – these types of residuals would, indeed manifest as high spatial frequency degradation, but would more likely show up further out in the PSF structure, or at least not completely destroy the diffraction structure outside the first airy ring. Investigation as to the origin and mitigation of these effects is prudent, and the potential for gain in image quality is on the order of 30% Strehl. Two suggested starting points, parameter space selection and initial control loop parameter calibration, are discussed below.

Explore Different Parameter Spaces

While it seems natural to use the Zernike polynomials for a circular (or annular) pupil, the deformable mirror does not morph smoothly over its disk. Each of the actuators behind the mirror push up and pull down and they are spaced at discreet points in a cartesian grid. Thus it may be useful to modulate the actuators in a parameter space that is more natural to them, rather than the shape of the pupil. This is especially true since there is evidence of high spatial

frequency aberrations in the default NCPA files, as well as the corrected ones, and thus it might be only corrected in Zernike space at very high orders, since the polynomial is infinite in nature. The "orthonormal mirror Zernike basis" used in shaping the DM represents well the first 136 Zernike terms, but after that the basis starts to break down[18], so even if value was seen in attempting to correct higher order terms, the corrections wouldn't see consistent results after z136.

There is evidence[5] that modulating the actuators in their own "actuator" space has been attempted in the past, although it is unknown if the work was ever completed or how successful it was. This approach may be useful to explore in the future, especially since there already exists some previously written code that could be used to study the approach. However, care must be taken to avoid falling into a local maximum, since the actuator space is not necessarily orthogonal over the wavefront at the pupil plane. In effect, the maximization of the image quality via the movement of a single actuator may be different depending on the configuration of the other actuators. One way to avoid falling into one of these "local maxima/ minima" traps is to start at a known point of decent image quality and use small adjustments.

Another approach may be to use a different orthogonal basis over the wavefront, such as a Fourier space, whereby actuators are moved in rows and columns along different frequency sine and cosine waves. This approach could be useful to attempt, although also could lead to "aliasing modes" when the spatial frequencies approach the distance between the actuators.

There are countless other parameter spaces that are orthogonal over an circular or annular aperture, and it is worth mentioning that this topic certainly warrants further research and investigation, although falls outside the scope of this paper.

Revisit Fundamental Calibration Parameters

One thing that may be worth examining is to return to the initial calibrations in the control loops that were determined and implemented circa 2003. Many adaptations have been made to the instrument since then, as well as collimation of the primary telescope optics and replacement of the secondary mirror, among other changes[28]. It could also be that the response of one or more of the actu-

---

[28]Degradation in image quality or control loop stabilization due to these two specific examples, while certainly relevant, would not have shown up in this experiment since those particular common-path optics were excluded.

ators has changed over time, and an updated interaction matrix is necessary – this may well be an "easy fix" if it is determined to be the cause of the problem. Refining the control loop parameters may have a significant effect on NCPA optimization, and it could very well be that some of the high spatial frequency aberrations are due to these control matrices and fundamental, deterministic parameters. If this is the case, it may be worth consultation with some of the experts who were involved in the building and commissioning of the instrument in order to both catalyze and increase chances for success.

4　Summary

Non-common path aberrations were suspected to be one of three significant causes of some notable image quality problems facing Gemini North's adaptive optics facility, Altair. This experiment attempted to mitigate this source of image degradation in daytime (and therefore less costly) conditions by employing focal plane sharpening techniques using a calibration source that is internal to Altair and imaging directly on the science detector. Two simple algorithms were examined: the simplex downhill approach and a simple "step-through" approach. In each case, the strehl ratio was measured directly on the science detector in the K-prime wavelength regime while varying the deformable mirror by sending Zernike coefficient changes to the control loops via the NCPA file. The step-through technique was shown to function appropriately both in terms of effectiveness and efficiency, and will be used to optimize the NCPA of other instruments and cameras that image through adaptive optics at Gemini North. An increase in Strehl ratio of about 6% was obtained using these techniques on NIRI in the f/32 camera at $2.12\mu m$, and most notably, $-0.15\mu m$ of $45^{\underline{o}}$ astigmatism has been mitigated. A potentially previously unknown and undiscovered problem was uncovered as well in the form of high spatial frequency degradations in the airy rings of the PSF of the calibration source and there is on the order of 30% Strehl ratio to be gained if sources for these degradations can be found and corrected. Work is ongoing to explore improvements and new approaches in the technique and also characterize and correct he NCPA of other instruments and imaging modes that are used with Altair at Gemini North.

A   Logged Comparison Data Pre- and Post-optimiztion to z37

```
--------------------------------------------------------------------------------
---------------COMPARING NEW (OPTIMIZED) NCPA FILE WITH PREVIOUS---------------
--------------------------------------------------------------------------------


Comparing aoNcpaNIRIp1Ngs.dat to aoNcpaTestFile.dat


Image Number | Measured Strehl Ratio | Zernike Coefficients (a)
------------   ---------------------   ------------------------
     493.000      0.478750       0.00000
     494.000      0.498269       0.00000
     495.000      0.481473       0.00000
     496.000      0.490382       0.00000
     497.000      0.471400       0.00000
     498.000      0.501335       0.00000
     499.000      0.496851       0.00000
     500.000      0.507616       0.00000
     501.000      0.491714       0.00000
     502.000      0.516616       0.00000
Mean Strehl with these Zernike coefficients is S~     0.493441    +/-    0.0137131

Image Number | Measured Strehl Ratio | Zernike Coefficients (a)
------------   ---------------------   ------------------------
     503.000      0.564467       0.00000
     504.000      0.524278       0.00000
     505.000      0.598047       0.00000
     506.000      0.521369       0.00000
     507.000      0.536206       0.00000
     508.000      0.578030       0.00000
     509.000      0.545726       0.00000
     510.000      0.550096       0.00000
     511.000      0.539374       0.00000
     512.000      0.563701       0.00000
Mean Strehl with these Zernike coefficients is S~     0.552129    +/-    0.0241494
```

Figure 15: Appendix A

Log data from the comparison of the default to the optimized strehl (Zernike coefficients are listed as zero because they are now included in the NCPA file used to generate the data, and therefore are not offset: the column header is a remnant of the formatting for data logs prior to the creation of the "Test" NCPA file.

50

B   Final Offset Coefficients to Default NIRI NCPA File to z37

Zernike Coefficient	Optimized value $\pm 0.01 \mu m$
z5	-0.14
z6	0.02
z7	0.00
z8	0.04
z9	0.02
z10	0.02
z11	0.00
z12	-0.02
z13	0.01
z14	0.03
z15	0.01
z16	-0.03
z17	-0.02
z18	-0.01
z19	0.00
z20	-0.02
z21	-0.01
z22	-0.01
z23	0.01
z24	0.00
z25	-0.01
z26	-0.02
z27	-0.02
z28	0.02
z29	0.01
z30	0.02
z31	0.01
z32	-0.02
z33	0.02
z34	0.00
z35	0.00
z36	0.00
z37	0.00

Table 2: Appendix B

Final, optimized offset Zernike mirror mode coefficient values (in micrometers) of NCPA file from the default.

C IDL Code Exerpts

C.1 "func" code

```
function func, a

common ncpaoptimizers, strehlinit, maxstrehl, imnum, sig, ni, funclog, ncpanom, lambda, dark

altairinitio,debug=1

if n_elements(strehlinit) eq 0 then strehlinit = 'n/a'
if n_elements(maxstrehl) eq 0 then maxstrehl = 'n/a'

print,'****************************************************************************'
print,'Opening guide loops and loading ncpa file...'
print,'****************************************************************************'

temp = altairOpenLoop()              ;from altairEpics.pro
wait,1

;Load the nominal ncpa file
if not keyword_set(ncpanom) then begin
    print,'Which NCPA file do you want to start with?'
    print,'1 -- NIRI (default)'
    print,'2 -- GMOS'
    print,'3 -- Zero'
    print,'4 -- Telescope'
    print,'5 -- Last Written Test File'
    read,ncpanom
    if ncpanom eq 1 then ncpanom = 'aoNcpaNIRIp1Ngs.dat'
    if ncpanom eq 2 then ncpanom = 'aoNcpaGMOSp5Ngs.dat'
    if ncpanom eq 3 then ncpanom = 'aoNcpaPar_zero.dat'
    if ncpanom eq 4 then ncpanom = 'aoNcpaZeroNgs.dat'
    if ncpanom eq 5 then ncpanom = 'aoNcpaTestFile.dat'
    spawn,'scp gemvx@pisces:/gemini/altair/altair/input/aoNcpaNIRIp1Ngs.dat aoNcpaNIRIp1Ngs.dat'
    spawn,'scp gemvx@pisces:/gemini/altair/altair/input/aoNcpaGMOSp5Ngs.dat aoNcpaGMOSp5Ngs.dat'
    spawn,'scp gemvx@pisces:/gemini/altair/altair/input/aoNcpaPar_zero.dat aoNcpaPar_zero.dat'
    spawn,'scp gemvx@pisces:/gemini/altair/altair/input/aoNcpaZeroNgs.dat aoNcpaZeroNgs.dat'
    spawn,'scp gemvx@pisces:/gemini/altair/altair/input/aoNcpaTestFile.dat aoNcpaTestFile.dat'
endif
temp = setncpa(ncpanom)

;Update the ncpa with the vector a
updateAoNcpaPar,a,fileIn=ncpanom,fileOut='ncpa_simplex.dat',gain=1,/nodisplay
spawn,'scp ncpa_simplex.dat gemvx@pisces:/gemini/altair/altair/input/ncpa_simplex.dat'
temp = setncpa('ncpa_simplex.dat')
temp = clickCreateNewControlMatrix()
wait,1

print,'****************************************************************************'
print,'Closing guide loops...'
print,'****************************************************************************'

;close the guide loops, take a NIRI image, and open the loops
temp = altairCloseLoop()             ;from altairEpics.pro

print,'****************************************************************************'
print, 'loop is closed, waiting to stabilize (16s)...'
print,'****************************************************************************'

wait, 16 ;wait 16 seconds to make sure loop stabilizes
print,'****************************************************************************'
print,'taking NIRI images...'
print,'****************************************************************************'

;TAKE A SERIES OF IMAGES AND GET A MEAN STREHL VALUE
if n_elements(ni) eq 0 then ni=1
tempstrehlarr = 0.
for i=0,ni-1 do begin
    if altairCaget('ao:correctM.VALA','i') ne 1 || altairCaget('ao:wfcs:getStatus2.VALM','i') ne 1 then begin
        temp = altairOpenLoop()
        wait,1
        temp = altairCloseLoop()
        wait,16
    endif
```

Figure 16: "func" code (pt. 1)

```idl
    temp = nirigo()
    lastfile = altaircaget('niri:dc:sad:dataLabel.VAL','s')
    imnum = fix(strmid(lastfile,10,4))

    if i lt ni-1 then begin
        print,'*************************************************************************'
        print,'image number  ',lastfile,'  acquired, analyzing...'
        print,'*************************************************************************'
        wait, 1
    endif

    ;Read in the NIRI image that was just taken and subtract the dark
    ;data may be found in either of the following directories (not sure which is better):
    ; /net/mko-nfs/sci/dataflow       OR
    ; /gemsoft/dhs/perm
    fits_read,'/gemsoft/dhs/perm/'+lastfile+'.fits', im
    im = im - dark

    ;crop image to mitigate "edge effects"
    xymax = findmax(im)
    ims=im(xymax(0)-64:xymax(0)+63,xymax(1)-64:xymax(1)+63)

    ;determine the background from the histogram (using the mode/ max hist is most accurate)
    nbin = 40
    histmax,im,res,nbin=nbin,vmin=-20,vmax=400,/fit
    bkg= res(0)

    print,'*************************************************************************'
    print, 'Background estimate is:__', bkg
    print,'*************************************************************************'

    wait,2

    if not keyword_set(lambda) then lambda = 2.12

    ;analyze the strehl ratio
    fwhmstrehl,sigma_filter(ims-bkg,3,n_sig=3,/all),0.021,lambda,7.9,0.13,strehl,fwhm,sab,/autoback,/debug

    print,'*************************************************************************'
    print, 'strehl ratio is:__',strehl
    print,'*************************************************************************'
    wait,2

    ;collect an array of strehl values and show them as they collect
    if n_elements(funclog) eq 0 then funclog = [imnum,strehl,a] else funclog = [[funclog],[imnum,strehl,a]]
    if n_elements(tempstrehlarr) le 1 && tempstrehlarr eq 0 then begin
        tempstrehlarr = strehl
        get_lun,lun
        openw,lun,'ncpaoptimize.log',/append,WIDTH=320  ;file will be located in /net/mko-nfs/gem/home/telops/perm/altair/idl/temp
        printf,lun,''
        printf,lun,'Image Number | Measured Strehl Ratio | Zernike Coefficients (a)'
        printf,lun,'------------   ---------------------   ------------------------'
        printf,lun, [imnum,strehl,a]
        close,lun
        free_lun, lun
    endif else begin
        tempstrehlarr = [tempstrehlarr, strehl]
        get_lun, lun
        openw,lun,'ncpaoptimize.log',/append,WIDTH=320  ;file will be located in /net/mko-nfs/gem/home/telops/perm/altair/idl/temp
        printf,lun, [imnum, strehl, a]
        close,lun
        free_lun, lun
    endelse

endfor

strehl = mean(tempstrehlarr)
sig = stdev(tempstrehlarr)

get_lun,lun
        openw,lun,'ncpaoptimize.log',/append,WIDTH=320  ;file will be located in /net/mko-nfs/gem/home/telops/perm/altair/idl/temp

        printf,lun,'Mean Strehl with these Zernike coefficients is S~',strehl,'   +/-',sig
        close,lun
        free_lun, lun

print,'*************************************************************************'
print,'Zernike Coefficients:'
print,a
print,'produce a mean strehl ratio of:'
print,strehl, ' +/-', sig
print,'*************************************************************************'

wait, 1

return, -strehl

end
```

Figure 17: "func" code (pt. 2)

The IDL function "func" represents the "heart" of the code used to do the majority of the work: take NIRI images, analyze the image quality, and implement NCPA correction files, along with writing output to various log files.

C.2 Simplex algorithm

```
pro NcpaSimplex

common ncpaoptimizers, strehlinit, maxstrehl, imnum, sig, ni, funclog, ncpanom, lambda, dark

strehlarr = 0.

;start a log file and open it in a new terminal
get_lun,lun
openw,lun,'ncpaoptimize.log',/append,WIDTH=320  ;file will be located in /net/mko-nfs/gem/home/telops/perm/altair/idl/temp
printf,lun,''
printf,lun,'--------------------------------------------------------------------------------'
printf,lun,'----------------------STARTING NEW NCPA OPTIMIZATION RUN----------------------'
printf,lun,'----------------------------------SIMPLEX METHOD-----------------------------'
printf,lun,'--------------------------------------------------------------------------------'
printf,lun,''
close,lun
free_lun, lun

yn = 'n'
print,'Would you like to open up a log file? (y/n)?'
read,yn
if yn eq 'y' then spawn,'xterm -hold -e tail -f ncpaoptimize.log &'

altairNiriNcpaInit        ;from altairNiriNcpa.pro

;load the nominal ncpa value into the local temp directory (i.e., a 'zero point')
print,'Which NCPA file do you want to start with?'
print,'1 -- NIRI (default)'
print,'2 -- GMOS'
print,'3 -- Zero'
print,'4 -- Telescope'
print,'5 -- Last Written Test File'
read,ncpanom
if ncpanom eq 1 then ncpanom = 'aoNcpaNIRIp1Ngs.dat'
if ncpanom eq 2 then ncpanom = 'aoNcpaGMOSp5Ngs.dat'
if ncpanom eq 3 then ncpanom = 'aoNcpaPar_zero.dat'
if ncpanom eq 4 then ncpanom = 'aoNcpaZeroNgs.dat'
if ncpanom eq 5 then ncpanom = 'aoNcpaTestFile.dat'
spawn,'scp gemvx@pisces:/gemini/altair/altair/input/aoNcpaNIRIp1Ngs.dat aoNcpaNIRIp1Ngs.dat'
spawn,'scp gemvx@pisces:/gemini/altair/altair/input/aoNcpaGMOSp5Ngs.dat aoNcpaGMOSp5Ngs.dat'
spawn,'scp gemvx@pisces:/gemini/altair/altair/input/aoNcpaPar_zero.dat aoNcpaPar_zero.dat'
spawn,'scp gemvx@pisces:/gemini/altair/altair/input/aoNcpaZeroNgs.dat aoNcpaZeroNgs.dat'
spawn,'scp gemvx@pisces:/gemini/altair/altair/input/aoNcpaTestFile.dat aoNcpaTestFile.dat'

print,'Enter the wavelength of the filter you are using.'
read,lambda

;set number of coefficients to correct, starting with Z5 (astigmatism)
;e.g., use 18 to go to z22
read, na, prompt = 'How many Zernike terms (starting with astigmatism -- Z5) should we include in the correction?  '
a0 = fltarr(na)
strehlinit = 0.

read, ni, prompt='How many images on each iteration would you like to average?'

;Run the optimization using the idl 'amoeba' function.
;scale is the overall size of the parameter space (use a vector if each term has a different expected parameter size)
;a0 is the starting point (usually all zeros). Should be a vector of Zernike coefficients starting with Z4, astigmatism
;tol is the tolerance. should be set to how precise we want the zernike coefficients to be

yn = 'n'
scale = 0.4
tol = 0.02
read, yn, prompt='Would you like to start with predetermined coefficients (y/n)?'
if yn eq 'y' then begin
    print,'Type in the coefficients separated by commas.'
    read,a0
    yn = 'n'
    print,'Would you like to set the scale used to locate the maximum strehl (i.e., how far away from the coefficients we look)?'
    print,'Default is',scale
    read,yn
```

Figure 18: "NcpaSimplex" procedure (part 1)

```
    if yn eq 'y' then begin
        yn = 'n'
        print,'Would you like to set individual scales for each coefficient?'
        read,yn
        if yn eq 'y' then begin
            scale = fltarr(na)
            print,'Enter the scales for each coefficient.'
            read,scale
        endif
        if yn eq 'n' then begin
            print,'Enter the scale.'
            read,scale
        endif
    endif
endif

;take a niri "dark" image (image without the cal source on) to subtract out the hot pixels
temp = altairOpenLoop()
altairCaput,'ao:selectCalMode.A','OFF'
altairCaput,'ao:selectCalMode.DIR','0'
altairCaput,'ao:selectCalMode.DIR','3'
wait,1
temp = nirigo()
lastfile = altaircaget('niri:dc:sad:dataLabel.VAL','s')
imnum = fix(strmid(lastfile,10,4))
fits_read,'/gemsoft/dhs/perm/'+lastfile+'.fits', dark
altairCaput,'ao:selectCalMode.A','ON'
altairCaput,'ao:selectCalMode.DIR','0'
altairCaput,'ao:selectCalMode.DIR','3'


a = amoeba(tol,scale=scale,p0=a0,function_value=strehl)

strehl = abs(strehl)
strehl = mean(strehl)

openw,lun,'ncpaoptimize.log',/append,WIDTH=320
printf,'***************************************************************************'
printf,'Initial strehl ratio was ',strehlinit
printf,'Corrected NCPA gives a maximum strehl ratio of',strehl
printf,'with the following coefficients (a) appended to the nominal NCPA file: '
printf, a
printf,'corresponding to an improvement in strehl ratio of approximately ', 100*(strehl-strehlinit)/strehlinit, 'percent! '
printf,'***************************************************************************'
close,lun
free_lun,lun


end
```

Figure 19: "NcpaSimplex" procedure (part 2)

The IDL procedure "NcpaSimplex" is one of the two "brain" pieces implemented that takes care of initializations, interpreting the IQ analysis given by "func", and varying the NCPA (Zernike coefficients) according to IDL's "amoeba" downhill simplex algorithm.

C.3 Step-through algorithm

```
pro ncpastep

common ncpaoptimizers, strehlinit, maxstrehl, imnum, sig, ni, funclog, ncpanom, lambda, dark

;start a log file and open it in a new terminal
get_lun,lun
openw,lun,'ncpaoptimize.log',/append,WIDTH=320  ;file will be located in /net/mko-nfs/gem/home/telops/perm/altair/idl/temp
printf,lun,''
printf,lun,'------------------------------------------------------------------------------------'
printf,lun,'-----------------------STARTING NEW NCPA OPTIMIZATION RUN-----------------------'
printf,lun,'-----------------------------------STEP METHOD------------------------------------'
printf,lun,'------------------------------------------------------------------------------------'
printf,lun,''
close,lun
free_lun, lun

yn = 'n'
print,'Would you like to open up a log file? (y/n)?'
read,yn
if yn eq 'y' then spawn,'xterm -hold -e tail -f ncpaoptimize.log &'

;Initialize Niri and Altair for the optimization
;Load an appropriate (i.e., nominal) NCPA file

altairNiriNcpaInit      ;from altairNiriNcpa.pro
spawn,'scp gemvx@pisces:/gemini/altair/altair/input/aoNcpaNIRIp1Ngs.dat aoNcpaNIRIp1Ngs.dat'
spawn,'scp gemvx@pisces:/gemini/altair/altair/input/aoNcpaGMOSp5Ngs.dat aoNcpaGMOSp5Ngs.dat'
spawn,'scp gemvx@pisces:/gemini/altair/altair/input/aoNcpaPar_zero.dat aoNcpaPar_zero.dat'
spawn,'scp gemvx@pisces:/gemini/altair/altair/input/aoNcpaZeroNgs.dat aoNcpaZeroNgs.dat'
spawn,'scp gemvx@pisces:/gemini/altair/altair/input/aoNcpaTestFile.dat aoNcpaTestFile.dat'
funclog = []           ;clear this variable

print,'Enter the wavelength of the filter you are using.'
read,lambda

;load the nominal ncpa value into the local temp directory (i.e., a 'zero point')
print,'Which NCPA file do you want to start with?'
print,'1 -- NIRI (default)'
print,'2 -- GMOS'
print,'3 -- Zero'
print,'4 -- Telescope'
print,'5 -- Last Written Test File'
read,ncpanom
if ncpanom eq 1 then ncpanom = 'aoNcpaNIRIp1Ngs.dat' else $
if ncpanom eq 2 then ncpanom = 'aoNcpaGMOSp5Ngs.dat' else $
if ncpanom eq 3 then ncpanom = 'aoNcpaPar_zero.dat' else $
if ncpanom eq 4 then ncpanom = 'aoNcpaZeroNgs.dat' else $
if ncpanom eq 5 then ncpanom = 'aoNcpaTestFile.dat' else ncpanom = 'aoNcpaNIRIp1Ngs.dat'

;Define the coefficient to optimize
print,'Which Zernike term do you want to optimize?'
print,'5 - Z5 (45 deg primary astigmatism)'
print,'6 - Z6 (0 deg primary astigmatism)'
print,'7 - Z7 (primary y coma)'
print,'8 - Z8 (primary x coma)'
print,'9 - Z9 (trefoil 1)'
print,'10 - Z10 (trefoil 2)'
print,'11 - Z11 (primary spherical)'
print,'etc., etc., etc.'
read, wa
wa = fix(wa)
na = wa-4                  ; number of elements in the a array
mode = wa-5                    ;coefficient of a that we are optimizing on this run
a0 = fltarr(na)            ;create an initial array of coefficients
yn=''
read,yn,prompt='Would you like to start with pre-determined coefficient offsets (y/n)?'
if yn eq 'y' then begin
    print,'Enter the initial Zernike coefficients (a0) separated by commas.'
    print,'Enter 0 for the coefficient that you are optimizing.'
    read,a0,prompt='a0 = '
endif
```

Figure 20: "ncpastep" procedure (part 1)

The IDL procedure "ncpastep" is another "brain" piece (the more successful one in this experiment) that takes care of initializations, interpreting the IQ analysis given by "func," and varying the NCPA (Zernike coefficients) by stepping through a given range to find the best image quality.

```
read, nstep, prompt = 'How many steps should we walk through the coefficient with (hint: use an odd number to avoid a redundant zero-point)? '
nstep = nstep-2
read, scale, prompt = 'How far away from zero should we vary the coefficients (i.e., define the range -- .5 is always a safe bet)? '
read, ni, prompt = 'How many images at each iteration (i.e., sample size) would you like to take?'

;start several log files
get_lun,lun
openw,lun,'ncpaoptimize.log',/append,WIDTH=320
printf,lun,''
printf,lun,'Wavelength = ' + string(lambda,format='(f0.2)') + ' um'
printf,lun,'Optimizing Z' + strtrim(string(wa),2) + ' with initial NCPA offsets of:'
for n = 0,na-1 do begin
    printf,lun,'Z' + strtrim(string(n+5),2) + ' = ' + strtrim(string(a0(n)),2)
endfor
printf,lun,''
close,lun
free_lun,lun

get_lun,lun
openw,lun,'stepfull.log',/append,WIDTH=320
printf,lun,''
printf,lun,'Wavelength = ' + string(lambda,format='(f0.2)') + ' um'
printf,lun,'Optimizing Z' + strtrim(string(wa),2) + ' with initial NCPA offsets of:'
for n = 0,na-1 do begin
    printf,lun,'Z' + strtrim(string(n+5),2) + ' = ' + strtrim(string(a0(n)),2)
endfor
printf,lun,''
printf,lun,''
printf,lun,'Image Number | Measured Strehl Ratio | Coefficient (Z' + strtrim(string(wa),2) + ')'
printf,lun,''
close,lun
free_lun,lun

get_lun,lun
openw,lun,'stepmean.log',/append,WIDTH=320
printf,lun,''
printf,lun,'Wavelength = ' + string(lambda,format='(f0.2)') + ' um'
printf,lun,'Optimizing Z' + strtrim(string(wa),2) + ' with initial NCPA offsets of:'
for n = 0,na-1 do begin
    printf,lun,'Z',strtrim(string(n+5),2) + ' = ' + strtrim(string(a0(n)),2)
endfor
printf,lun,''
printf,lun,''
printf,lun,'Mean Strehl Ratio | Standard Deviation | Coefficient (Z' + strtrim(string(wa),2) + ')'
printf,lun,''
close,lun
free_lun,lun

;step through a curve for the specified zernike term in order to find the maximum strehl for that term

;take a niri "sky" image (image without the cal source on) to subtract out the hot pixels
temp = altairOpenLoop()
altairCaput,'ao:selectCalMode.A','OFF'
altairCaput,'ao:selectCalMode.DIR','0'
altairCaput,'ao:selectCalMode.DIR','3'
wait,1
temp = nirigo()
lastfile = altaircaget('niri:dc:sad:dataLabel.VAL','s')
imnum = fix(strmid(lastfile,10,4))
fits_read,'/gemsoft/dhs/perm/'+lastfile+'.fits', dark
altairCaput,'ao:selectCalMode.A','ON'
altairCaput,'ao:selectCalMode.DIR','0'
altairCaput,'ao:selectCalMode.DIR','3'

;take an initial strehl measurement with nominal ncpa correction
strehlarr = 0.
strehlinit = 0.
maxstrehl = 0.
maxstrehlarr = 0.
stepfull = 0.
```

Figure 21: "ncpastep" procedure (part 2)

```
a = a0
tempstrehl = abs(func(a))
strehlinit = tempstrehl

stepmean = [tempstrehl,sig,a(mode)]
get_lun,lun
openw,lun,'stepmean.log',/append,WIDTH=320
printf,lun,tempstrehl,sig,a(mode)
close,lun
free_lun,lun

;initialize some arrays
meanstrehlarr = fltarr(nstep+2)
meanstrehlarr(0) = tempstrehl
sigarr=fltarr(nstep+2)
sigarr(0)=sig

;step through and take images, log the output
asteps=(findgen(nstep)-(nstep/2.))*((scale*2.)/(nstep))
asteps=[0,asteps,scale]
for step=1,nstep+1 do begin
    a(mode)=asteps(step)
    tempstrehl = abs(func(a))
    sigarr(step) = sig
    meanstrehlarr(step)=tempstrehl

    get_lun,lun
    openw,lun,'stepmean.log',/append,WIDTH=320
    printf,lun,tempstrehl,sig,a(mode)
    close,lun
    free_lun,lun
endfor

;sort the order of the various arrays according to the increments of the coefficeints (i.e., step number)
index=sort(asteps)
asteps=asteps(index)
meanstrehlarr=meanstrehlarr(index)
sigarr=sigarr(index)

;create a results matrix
resultarr = [[asteps],[meanstrehlarr],[sigarr]]

finesteps = (findgen(200)-100)*((scale*2.)/200)
finesteps = [finesteps,scale]
result=poly_fit(asteps,meanstrehlarr,2)                           ;fit a parabola to the data
a = a0
a(mode)=-result(1)/(2*result(2))                                 ;find coefficient that maximizes the strehl
strehlfit = result(0)+result(1)*finesteps+result(2)*finesteps^2        ;plot the results and the fit
maxstrehlfit = result(0)+result(1)*a(mode)+result(2)*a(mode)^2        ;find max strehl from curve fit
plot, asteps, meanstrehlarr, psym=1
oplot, finesteps, strehlfit
print,'Maximum Strehl (measured) = ', max(abs(meanstrehlarr))
print,'Maximum Strehl (inferred) = ', maxstrehlfit
print,'Zernike coefficients (a) = ', a

;update test ncpa file with the new coefficients
yn = 'n'
print,'Do you want to update the Test NCPA file with this optimized coefficient?'
read,yn
if yn eq 'y' then begin
    spawn,'scp gemvx@pisces:/gemini/altair/altair/input/aoNcpaTestFile.dat aoNcpaTestFile.revert.dat'
    updateAoNcpaPar,a,fileIn=ncpanom,fileOut='aoNcpaTestFile.dat',gain=1,/nodisplay
    spawn,'scp aoNcpaTestFile.dat gemvx@pisces:/gemini/altair/altair/input/aoNcpaTestFile.dat'
endif

;output to logs
get_lun,lun
openw,lun,'stepfull.log',/append,WIDTH=320
printf,lun,funclog
printf,lun,''
printf,lun,'*****************************************************************************'
printf,lun,'Maximum strehl ratio expected is S ~' + strtrim(string(maxstrehlfit),2)
;printf,lun,'The strehl is maximized when Z' + strtrim(string(wa),2) + ' = ' + strtrim(string(a(mode)),2)
printf,lun,'With total Zernike coefficient contributions, starting at Z5 (astigmatism) of a = ',a
printf,lun,'*****************************************************************************'
close,lun
free_lun,lun

get_lun,lun
openw,lun,'stepmean.log',/append, WIDTH=320
printf,lun,''
printf,lun,'*****************************************************************************'
printf,lun,'Maximum strehl ratio expected is S ~' + strtrim(string(maxstrehlfit),2)
;printf,lun,'The strehl is maximized when Z' + strtrim(string(wa),2) + ' = ' + strtrim(string(a(mode)),2)
printf,lun,'With total Zernike coefficient contributions, starting at Z5 (astigmatism) of a = ',a
printf,lun,'*****************************************************************************'
close,lun
free_lun,lun

get_lun,lun
openw,lun,'ncpaoptimize.log',/append,WIDTH=320  ;file will be located in /net/mko-nfs/gem/home/telops/perm/altair/idl/temp
printf,lun,'*****************************************************************************'
printf,lun,'Initial strehl ratio was ',strehlinit
printf,lun,'Corrected NCPA calculates a maximum strehl ratio of',maxstrehlfit
printf,lun,'with the following coefficients (a) appended to the nominal NCPA file: '
printf,lun, a
printf,lun,'corresponding to an improvement in strehl ratio of approximately '+ strtrim(string(100*(maxstrehlfit-strehlinit)/strehlinit),2) + 'percent! '
if yn eq 'y' then begin
    printf,lun,'aoNcpaTestFile.dat has been updated with these optimized coefficients'
endif
if yn eq 'n' then begin
    printf,lun,'aoNcpaTestFile.dat has NOT been updated with these optimized coefficients.'
endif
printf,lun,'*****************************************************************************'
close,lun
free_lun, lun

end
```

Figure 22: "ncpastep" procedure (part 3)

References

[1] Lai, Olivier, Jean-Pierre Véran, Glen Herriot, John White, Jesse Ball, and Chad Trujillo. "Altair Performance and Upgrades." Adaptive Optics Systems IV (2014): Web.

[2] Roddier, F. *Adaptive Optics in Astronomy.* Cambridge, U.K.: Cambridge UP, 1999. Print.

[3] Lamb, Masen, David R. Andersen, Jean-Pierre Véran, Carlos Correia, Glen Herriot, Matthias Rosensteiner, and Jason Fiege. "Non-common Path Aberration Corrections for Current and Future AO Systems." Adaptive Optics Systems IV (2014): Web.

[4] Press, William H., and William H. Press. "Chapter 10. Minimization or Maximization of Functions." *Numerical Recipes in FORTRAN*: *The Art of Scientific Computing.* Cambridge: n.p., 1992. Web.

[5] Rigaut, François. "Altair Man Pages." Altair Man Pages. Gemini Observatory, 1 May 2004. Web.

[6] Christou, Julian. "Image Processing and Deconvolution." Summer School on Adaptive Optics 2004. UCSC CfAO, Santa Cruz, CA. Year 3 in Review. Web. <http://cfao.ucolick.org/aosummer/archive/aosummer2004/pdf/ChristouDeconv.pdf>.

[7] "Gemini Observatory: Exploring The Universe, Sharing Its Wonders." Telescopes and Sites. Web. <http://www.gemini.edu/node/10750>.

[8] Tokovinin, A. "3. Wavefront Sensors." Web. <http://www.ctio.noao.edu/~atokovin/tutorial/part3/wfs.html>.

[9] "Principles of Wavefront Sensing and Reconstruction." Web. <http://cfao.ucolick.org/aosummer/book/pdf/1.1_chanan.pdf>.

[10] Hodapp, Klaus W., Joseph B. Jensen, Everett M. Irwin, Hubert Yamada, Randolph Chung, Kent Fletcher, Louis Robertson, Joseph L. Hora, Douglas A. Simons, Wendy Mays, Robert Nolan, Matthieu Bec, Michael Merrill, and Albert M. Fowler. "The Gemini Near-Infrared Imager (NIRI)." PUBL ASTRON SOC PAC Publications of the Astronomical Society of the Pacific 115.814 (2003): 1388-406. Web.

[11] Herriot, Glen, Simon Morris, Scott C. Roberts, J. Murray Fletcher, Leslie K. Saddlemyer, Gurjeet Singh, Jean-Pierre Veran, and Eric H. Richardson. "Innovations in Gemini Adaptive Optics System Design." Adaptive Optical System Technologies (1998), Web.

[12] Saddlemyer, Leslie K., Glen Herriot, Jean-Pierre Veran, and J. Murray Fletcher. "Design Aspects of the Reconstructor for the Gemini Adaptive Optics System (Altair)." Adaptive Optical System Technologies (1998): n. pag. Web.

[13] Stephens, Andrew. "Gemini Observatory: Exploring The Universe, Sharing Its Wonders." NIRI. Gemini Observatory, Web.

[14] Trujillo, Chad. "Gemini Observatory: Exploring The Universe, Sharing Its Wonders." ALTAIR. Gemini Observatory, Web.

[15] Rigaut, François. "Altair Weblog." Gemini Observatory, Web. <http://internal.gemini.edu/science/instruments/Altair/blog/>.

[16] Gratadour, Damien, Eric Gendron, Gérard Rousset,. "Practical issues with phase diversity for NCPA compensation resolved on the CANARY demonstrator." Web. <http://ao4elt3.arcetri.astro.it/proceedings/fulltext_13325.pdf>

[17] Christou, Julian C., Benoit Neichel, Francois Rigaut, Michael Sheehan, Richard M. Mcdermid, Gelys Trancho, Chadwick Trujillo, and Brian Walls. "ALTAIR Performance and Updates at Gemini North." Adaptive Optics Systems II (2010): n. pag. Web.

[18] Veran, Jean-Pierre. Altair's Optimiser. Gemini Observatory

[19] Tokovinin, A. "AO Tutorial 3: Wave-front Sensors." Web. <http://www.ctio.noao.edu/~atokovin/tutorial/part3/wfs.html>.

[20] Mathar, R. J. "A176988 - OEIS." A176988 - OEIS. The OEIS Foundation, 8 Dec. 2010. Web. <https://oeis.org/A176988>.